electrolyte.[14,41] The large degree of disorder in these phases results in the entropy of fusion being unusually small. This explains why the initial slopes of the melting curves of especially CuI I, CuI VII, and CuBr I are extremely large, although the volume changes upon fusion are not unusually large. It is obvious that this behavior is not necessarily restricted to the α-AgI structures of CuBr I and CuCl III, but can also apply in the case of the disordered fcc defect structure of CuI I.

[41] J. Krogh-Moe, Selected Topics in High-Temperature Chemistry (unpublished).

ACKNOWLEDGMENTS

The authors would like to thank Mrs. Martha C. Pistorius for writing the computer programs used in fitting the data, Dr. G. Gafner and R. J. Murphy for valuable discussions, and J. B. Clark for assistance with much of the experimental work. J. Erasmus and his staff and G. O'Grady and his staff kept the equipment in good repair, and were responsible for the manufacture of the furnace parts. Calculations were carried out on the IBM System 360 of the National Research Institute for Mathematical Sciences.

PHYSICAL REVIEW VOLUME 172, NUMBER 3 15 AUGUST 1968

Vibrational Structures Accompanying the Optic Transitions of Bound Electrons in Crystals*†

E. MULAZZI, G. F. NARDELLI, AND N. TERZI

Istituto di Fisica dell'Università, and Gruppo Nazionale di Struttura della Materia del Consiglio Nazionale delle Ricerche, Milano, Italy

(Received 14 September 1967; revised manuscript received 22 January 1968)

A description of the phonon processes involved in the optic transitions of a bound electron in crystals is presented, with the specific properties of the electron-phonon interactions considered in detail. The set of forces that the "hole-electron pair" exerts on the surrounding lattice are used as coupling constants, and the projected density of states for the perturbed phonon field is fully explained. The orbit radii for the optic electron are assumed to be of the order of, or smaller than, the lattice parameter, and both dipole-allowed and electric-dipole phonon-forced transitions are considered. Short- and long-range forces are examined. The connection between short-range forces and the stress coefficients of the absorption (emission) band is found. The symmetry properties of the electron wave functions are further taken into account in the analysis of electrostatic types of interactions. It is shown that the electric dipole forces activate essentially the normal modes of the perfect lattice, while the short-range forces activate more easily the possible local and pseudolocal modes. An explanation is also suggested for the intraconfiguration transition of rare-earth ions not activating the pseudolocal modes. The Huang-Rhys parameter is split into local (pseudolocal) and continuum-mode terms. It is shown that the continuum-mode term prescribes how the total intensity of the band is shared among multiple-phonon lines (if present) and broad background absorption. The configuration-diagram description of the many-phonon process is subsequently considered, including the exciton absorption. An interpretation is presented of the Stokes shift between absorption and emission bands: The whole Stokes shift is split into a purely Stokes term and a stored-energy term, the latter being related to the infrared component $\mathbf{P}(\mathbf{r})$ of the polarization field. This purely Stokes term, as well as the phonon contribution to the peak position, is evaluated for the F band, within the linear and quadratic approximations for the electron-phonon interaction. Finally, a qualitative explanation is suggested for the Urbach rule in Perovskite-type crystals.

INTRODUCTION

THE absorption (emission) coefficient in the visible and uv region due to the optic transitions of a bound electron in crystals has been the subject of extensive research both from a theoretical[1–4] and from an experimental point of view.[5,6] It seems therefore

* This research has been sponsored in part by EOAR under Grants No. 65-05 and No. AF-EOAR 67-8 with the European Office of Aerospace Research, U. S. Air Force.

† A preliminary account of this work was presented at the Conference on Electronic and Ionic Properties of Alkali Halides, Milan, July, 1966 and appeared in *Proceedings of the Conference on Electronic and Ionic Properties of Alkali Halides*, edited by R. Fieschi and G. Spinolo (Gruppo Nazionale di Struttura della Materia, Istituto di Fisica dell'Università, Milan, Italy, 1966).

[1] M. Lax, J. Chem. Phys. **20**, 1752 (1952). The first analysis of the many-phonon process was given by W. E. Lamb, Phys. Rev. **55**, 190 (1939) in connection with neutron scattering.

[2] G. Rickayzen, Proc. Roy. Soc. (London) **A241**, 480 (1957).

[3] Yu. E. Perlin, Usp. Fiz. Nauk **80**, 553 (1964) [English transl.: Soviet Phys.—Usp. **6**, 542 (1964)]; this paper contains extensive references to previous works; D. McCumber, J. Math. Phys. **5**, 221 (1964), **5**, 508 (1964). For the connections with the Mössbauer effect, see, for instance: E. A. Trifonov, Fiz. Tverd. Tela **6**, 462 (1964) [English transl.: Soviet Phys.—Solid State **6**, 366 (1964)]; A. A. Maradudin, P. A. Flinn, and J. M. Radcliffe, Ann. Phys. N. Y. **26**, 81 (1964).

[4] M. H. L. Pryce, in *Phonons in Perfect Lattices and Lattices with Point Imperfections*, edited by R. W. H. Stevenson (Oliver and Boyd, Ltd., Edinburgh, 1966).

[5] D. B. Fitchen, R. H. Silsbee, T. A. Fulton, and E. L. Wolf, Phys. Rev. Letters **11**, 275 (1963); C. B. Pierce, Phys. Rev. **135**, A83 (1964). A. E. Hughes, Proc. Phys. Soc. (London) **87**, 535 (1966). For molecular centers see, for instance, T. Timusk and W. Staude, Phys. Rev. Letters **13**, 373 (1964). These papers represent just a sample.

[6] M. Wagner and W. E. Bron, Phys. Rev. **139**, A223 (1965); **139**, A233 (1965); W. E. Bron, *ibid.* **140**, A2005 (1965).

superfluous to spend too many words introducing this matter. In spite of these efforts, it seems to us that an important aspect of the problem, namely, the large variety of vibrational structures existing in the absorption (emission) bands and their connection with specific properties of the coupled electron-phonon system, remains unclear. Our purpose here is to clarify this point. It is well known[7] that the distribution function $I(\Omega)$ of the absorption (emission) band is related, in a simple way, to the spectral density, say $A(\Omega)$, of the thermodynamic Green function $\langle\langle\mathfrak{M}(t),\mathfrak{M}(0)\rangle\rangle_T$ for the electric dipole moment $\mathfrak{M}$ of the electron undergoing the optical transition. (Ω is the frequency of the electromagnetic field.) We have

$$I(\Omega)=KA(\Omega),$$

$$A(\Omega)=\mathrm{Im}\int_{-\infty}^{+\infty}dt\,e^{i\Omega t}\langle\langle e^{iHt}\mathfrak{M}e^{-iHt}\mathfrak{M}\rangle\rangle_T, \qquad (1)$$

where K is a smooth function of Ω which can be regarded as a constant factor in the range of frequencies that we are considering here. $\langle\langle\cdots\rangle\rangle_T$ denotes the thermal average at the absolute temperature T, and H denotes the total Hamiltonian of the interacting electron-phonon system. Equation (1) can be written in a simple way if we assume that the adiabatic approximation holds for the ground electronic state, as well as the excited states involved in the optic transition. In such a case, the distribution function as given by relation (1) is found, after some manipulations, to have essentially the standard form found in the literature [see Eqs. (5–3) and (5–18) Perlin's paper].[3] However, in order to reach a theoretical expression which permits a detailed interpretation of the phonon processes involved in the optic transition, a proper choice of the coupling constants for the electron-phonon interaction is critical. Usually, one introduces the set of normal-mode displacements Δ_λ. This leads to a description in which the peculiarities of the electron-phonon interaction are not separated from the specific properties of the imperfect-lattice dynamics. Furthermore, the electronic excitation involved in the optic response of the imperfect (perfect) crystal consists of a hole-electron pair. Instead of Δ_λ, we use the set of forces that this hole-electron pair exerts on the surrounding lattice. This allows us to introduce the projected density of states[8] of the perturbed (unperturbed) phonon field, and so to recognize clearly how the imperfect-lattice dynamics enters the description of the phonon process. Throughout the rest of this paper, we will refer to the interaction between the hole-electron pair and the phonons as the "electron-phonon interaction."

[7] V. L. Bonch-Bruevich, in *Green-Function Method in Statistical Mechanics* (North-Holland Publishing Co., Amsterdam, 1962).

[8] T. Timusk and M. V. Klein, Phys. Rev. 141, 664 (1966).

I. COUPLING CONSTANTS

We choose a representation in which the electron Hamiltonian occurs in matrix notation, while the lattice displacements $\mathbf{u}_{l\kappa}$ appear still in operator form. We use the pair indices l,κ to label the ions in the crystal: l labels N primitive cells and κ the ions within the primitive cell. We start with the lattice at elastic equilibrium (relaxed configuration) with respect to the initial level of the electron, and we assume that the wave function of any other level has been evaluated in this lattice configuration. The orbit radii of these electron wave functions are typical parameters of the centers which we are studying. Thus, a classification of the centers on the basis of the size of their electronic orbit radii, in both the initial and final states, allows us to determine the following three classes: (a) tightly bound electrons, when $r_u\sim r_g<r_a$, (b) weakly bound electrons, when $r_u\sim r_g\gg r_a$, (c) intermediate bonding, when $r_g\lesssim r_a$, but $r_u>r_a$.

By r_g and r_u, we have denoted the orbit radii of the initial and final electronic levels, $|\phi_g\rangle$ and $|\phi_u\rangle$, respectively, between which the transition occurs, and by r_a the radius of the equivalent sphere for the crystal atomic volume. Typical examples for the three classes are: the rare-earth ions and molecular centers, such as NO_2 in alkali halides, for class (a) electrons; shallow impurities in silicon and germanium and, to a lesser extent, complex centers in alkali halides such as R, M, and N centers for class (b) electrons; the F center in alkali halides and perhaps the intrinsic exciton for class (c) electrons.

We consider further the point symmetry of the defect; we call: "high-symmetry centers," the defects that possess inversion symmetry; "low-symmetry centers," the remaining defects. Finally, for class (a) electrons we consider the spectral terms which can be assigned to the optic transition of the free ion. Particular care must be taken in dealing with spin-orbit coupling. The d-like orbitals are considerably affected by the crystal field, and so the electronic levels must be classified first according to the irreducible representations (irr. reps.) of the crystal point group, and second according to the spin-orbit interaction. For f-like orbitals, the situation is reversed, since the crystal field represents only a small perturbation on the perturbation due to the spin-orbit coupling. In this case, and for high-symmetry centers, the total angular momentum can again be considered a good quantum number.

We consider next the electron wave functions in the vibrating lattice in the framework of the adiabatic principle. We develop the set of adiabatic wave functions in terms of the rigid-lattice wave functions $|\phi_i\rangle$, with coefficients which depend on the direct interaction between optic electron and phonons (i denotes an electron quantum number). The electron-phonon interaction consists of two types of terms: terms that are diagonal in the electron quantum numbers and terms

that are not. Since the lattice is supposed to be in elastic equilibrium in the initial state, for this state we include in the lattice Hamiltonian only the "diagonal part" of the electron-phonon interaction. We call $\Phi^{(g)}=\Phi_0+\delta\Phi$ the force-constant matrix of the imperfect lattice for this electronic level: $\delta\Phi$ accounts for the perturbation on the force constants due to the defect, which enters with the perturbation δM on the masses, into the definition of the frequency-dependent perturbation $\Lambda(\omega^2)$ (see Appendix A). We call $\Lambda(\omega^2)$ the lattice-dynamics perturbation.

A. Linear Coupling

We further analyze, in powers of lattice displacements $\mathbf{u}_{l\kappa}$ from the g-state equilibrium position $\mathbf{x}_{l\kappa}$, the additional perturbation which occurs in the lattice Hamiltonian once an electronic transition to another level (i.e., u) has occurred. The linear term is diagonal in electron quantum numbers g and u, and is of the form,

$$\sum_{l\kappa}\mathbf{f}_{l\kappa}\cdot\mathbf{u}_{l\kappa}. \tag{2}$$

As the electronic excitation consists of a hole-electron pair, in rigid-ion approximation, we write

$$\mathbf{f}_{l\kappa}=(\mp)\langle\phi_u|\frac{\partial}{\partial\mathbf{x}_{l\kappa}}V(\mathbf{r}-\mathbf{x}_{l\kappa})|\phi_u\rangle \\ (\pm)\langle\phi_g|\frac{\partial}{\partial\mathbf{x}_{l\kappa}}V(\mathbf{r}-\mathbf{x}_{l\kappa})|\phi_g\rangle, \tag{3}$$

where $V(\mathbf{r})$ is the effective potential, including the exchange, for the electron–host-lattice interaction. Equation (3) is seen to be nothing other than the force that the (trapped) hole-electron pair exerts on the $(l\kappa)$ ion. The upper sign refers to absorption, the lower to emission.

We call attention to the fact that for two definite electron levels, such as u and i, the linear "nondiagonal" (nd) part of the electron-phonon interaction is

$$\sum_{l\kappa}\mathbf{f}_{l\kappa}^{(ui)}\cdot\mathbf{u}_{l\kappa}, \tag{4}$$

where

$$\mathbf{f}_{l\kappa}^{(ui)}=-\langle\phi_u|\frac{\partial}{\partial\mathbf{x}_{l\kappa}}V(\mathbf{r}-\mathbf{x}_{l\kappa})|\phi_i\rangle, \tag{5}$$

and $\mathbf{f}_{l\kappa}^{(ui)}$ is the force that mixes together the pure states $|\phi_i\rangle$ and $|\phi_u\rangle$. We shall be concerned with the linear nd term mainly in dealing with the electric-dipole phonon forced transitions. Here we focus attention on the tightly bound electrons; however, the following considerations may also be applied to the intermediate bonding.[9]

We choose $\mathbf{f}_{l\kappa}$ and $\mathbf{f}_{l\kappa}^{(ui)}$ as the coupling constants for the linear terms of the electron-phonon interaction. Both fields split as:

$$\left\{\begin{matrix}\mathbf{f}_{l\kappa}\\ \mathbf{f}_{l\kappa}^{(ui)}\end{matrix}\right\}=[e_\kappa\mathbf{E}(\mathbf{x}_{l\kappa})-\mathbf{F}(\mathbf{x}_{l\kappa})], \tag{6}$$

where $\mathbf{E}(\mathbf{x}_{l\kappa})$ is the Coulomb part of the field, and $\mathbf{F}(\mathbf{x}_{l\kappa})$ the force coming from the exchange interaction between the electron and the $(l\kappa)$ ion. e_κ is the electric charge of the ions.

$\mathbf{F}(\mathbf{x}_{l\kappa})$ depends on the change of the overlapping integrals as well as on the rearrangement of electron spin in the optic transition. For tightly bound electrons it displays a marked short-range character.

$\mathbf{E}(\mathbf{x}_{l\kappa})$ can be expressed as a multipole expansion[6]; we retain terms up to the quadrupole. The *monopole* never occurs in the "nondiagonal" part of the electron-phonon interaction; it may occur in the "diagonal" part, thus contributing, together with a screening factor, to the change of local effective charge. It is again absent for tightly bound electrons, as the hole cancels the monopole term coming from the electron. The dipole and quadrupole depend more markedly on symmetry. First of all, we consider the *dipole* term. Let us denote by $\mathbf{p}$ the dipole moment which the optic transition switches in the impurity ion. At a distance $|\mathbf{R}|>(r_g,r_u)$ the dipole field reads

$$\mathbf{E}^{(d)}(\mathbf{R})=R^{-3}\mathbf{p}\cdot(3R^{-2}\mathbf{RR}-\mathbf{1}),$$

so that its contribution to the force $\mathbf{f}_{l\kappa}$ can be written as[10]

$$e_\kappa\mathbf{E}^{(d)}(\mathbf{x}_{l\kappa})/M_\kappa{}^{1/2}=\mathbf{d}\cdot\mathbf{L}_0{}^C(l\kappa;l'=0,\kappa')M_{\kappa'}{}^{1/2}, \tag{7}$$

where $\mathbf{d}\equiv(\mathbf{p}/e_\kappa)$; M_κ is the mass of the κth ion of the host crystal (M_0 in matrix notation). $\mathbf{L}_0{}^C(l\kappa,l'\kappa')$ is the Coulomb part of the dynamical matrix for the host lattice and we have put the defect at the origin $(l'=0,\kappa')$. This equation will be useful later. In high-symmetry centers, the dipole force transforms according to irr. reps. of odd parity. Then the dipole force enters only into the nondiagonal part of the interaction, $\mathbf{f}_{l\kappa}{}^{ui}$, insofar as we are concerned with electron wave functions u and i of opposite parity. For tightly bound electrons, a high-symmetry crystal field is not able to relax the selection rule $\Delta J=(0)\pm1$ of the free ion. Thus it is essentially the dipole force that allows the (dipole-forbidden) $(J=0)_{g(u)}\rightarrow(J=0)_{u(g)}$ transition. Wave functions, which indeed correspond to spectroscopic terms of total angular momentum, $J=0$, do not give rise for symmetry reasons to any quadrupole or higher multipoles in the diagonal part. Therefore, the Coulomb field contributes to the electron-phonon inter-

[9] Y. Toyozawa [Tech. Rept. of the Institute for Solid State Physics, Tokyo University, Ser. A, No. 238 (1967) (unpublished)] has recently proposed to use the deformation potential for the projection of $|f\rangle$ onto acoustic phonons and the Frolich interaction for the projection of $|f\rangle$ onto optic phonons [see also A. Myszkowski and S. Gomulka, Phys. Rev. 134, A1102 (1964)]. It seems to us that Toyozawa's approach is quite unrealistic for tightly bound electrons in polar crystals, and leads to wrong conclusions about the long-time behavior of the form factor, i.e., the behavior near the zero-phonon line of the response function (see the end of Sec. IIB).

[10] E. W. Kellermann, Phil. Trans. Roy. Soc. (London) A238, 513 (1940).

TABLE I. Field of force entering the diagonal and nondiagonal part of the electron-phonon interaction.

	High-symmetry centers		Low-symmetry centers
	diagonal interaction (f_{lk})	nondiagonal interaction (f_{lk}^{ui})	diagonal and nondiagonal interactions
tightly bound electrons $r_g \sim r_u \lesssim r_a$	quadrupole	dipole[a] quadrupole[b]	dipole and quadrupole (dipole only, if $J=0$)
intermediate bonding $r_g \lesssim r_a$ $r_u > r_a$	screened monopole, quadrupole, exchange	dipole[a] quadrupole[b]	screened monopole, dipole and quadrupole, exchange

[a] If the electron wave functions u and i have opposite parity.
[b] If the electron wave functions u and i have the same parity.

action only through the dipole term in the nondiagonal part. In low-symmetry centers, the crystal field relaxes the free-ion selection rules, and the dipole force enters into the diagonal and the nondiagonal parts of the interaction. In such a case, the (intraconfigurational) transition $(J=0)_{g(u)} \rightarrow (J=0)_{u(g)}$ of tightly bound electrons becomes dipole-allowed, because the low-symmetry crystal field mixes $J=0$ with $J=1$.

We should consider now the *quadrupole* force. However, we do not enter into its analysis in detail, since a theoretical approach can be found in Ref. 6. In high-symmetry centers, the quadrupole force transforms according to even representations. If we are then concerned with wave functions of the same parity, only the quadrupole force enters into both the "diagonal" and the "nondiagonal" forces.

Concerning the exchange interaction, we simply remark that the largest correction upon the Coulomb field is expected for class (c) electrons (i.e., intermediate coupling), because there the overlapping integral undergoes the maximum change in the optic transition. Fortunately, in this case, the coupling constants can be deduced from the stress coefficients of the band,[11,12] as shown in Sec. VB.

For both tightly bound and weakly bound electrons, only small corrections are expected, mainly to the short-range part of the fields.

Let us now briefly consider weakly bound electrons. For such electrons, a deformation-potential approach, recently suggested by Toyozawa,[9] is, in principle, more reliable than the rigid-ion approximation we have used in deriving Eqs. (3) and (5). However, we have to keep in mind that the phonon coupling for a hole-electron pair actually involves the difference between such deformation potentials for ground (upper) and upper (ground) states, respectively, of the optic electron. Unfortunately, when the electron orbit radii cover several interionic spacings, it is not clear how to differentiate between the deformation potentials for these two states. Small phonon coupling is, however, expected for the hole-electron pair, even if the electron-phonon coupling for the electron itself is fairly large. The situation is summarized in Table I.

We find it very useful to classify the optic transitions according to the extent of the force field $\mathbf{f}_{lk}$ in comparison with the region over which the lattice-dynamics perturbation $\Lambda(\omega^2)$ on the initial state is significantly different from zero. In this paper, we are only studying isoelectronic centers, so that monopole terms do not contribute to $\Lambda(\omega^2)$; any other long-range terms, such as the dipolar one, will be neglected here, since it is usually very small when compared with that coming from the short-range part of the ion-ion interaction. Therefore, $\Lambda(\omega^2)$ will be considered henceforth as a finite-range perturbation.

We use lable I to specify the subregion of the linear vector space (see Appendix) where $\Lambda(\omega^2)$ has nonvanishing matrix elements, and label II to denote the remaining space.

We split the field of force as

$$|f)=|f_{\mathrm{I}})+|f_{\mathrm{II}}),$$

where (see Appendix)

$$|f_{\mathrm{I}})=\sum_{\alpha j}|\mathrm{I};\alpha j)f_{\mathrm{I},\alpha j}, \tag{8}$$

and

$$|f_{\mathrm{II}})=\sum_{\alpha j}|\mathrm{II};\alpha j)f_{\mathrm{II},\alpha j}.$$

The label α denotes the irr. reps. of the point group.

Then we have: (*i*) *Short-range interaction.* The optic transition does not switch on any significant field of electric dipole in the lattice, and the upper-state wave function does not appreciably extend beyond the region (I). In this case $f_{\mathrm{II},\alpha j} \sim 0$ and we have only to consider the short-range part, i.e., $f_{\mathrm{I},\alpha j}$, of the electron-phonon interaction. (*ii*) *Long-range interaction.* Either the optic transition gives rise to an electric dipole field, or the upper-state wave function extends appreciably beyond region (I). This case requires a careful analysis of the field of force in both regions (I) and (II); nevertheless, a particularly simple situation occurs when the electron-phonon interaction is dominated by the long-range part, i.e., $f_{\mathrm{II},\alpha j}$, of the field of force. In such a case, we resort to the wave-vector representation, and we consider $(s\mathbf{q}|f)=f_{s\mathbf{q}}$, where $|\mathbf{q}s)$ denotes the unperturbed lattice wave of wave vector $\mathbf{q}$ and vibrational

[11] C. H. Henry, S. E. Schnatterly and C. P. Slichter, Phys. Rev. **137**, A583 (1965); S. E. Schnatterly, *ibid.* **140**, A1374 (1965); W. Gebhart and T. Meier, Phys. Status Solidi **8**, 303 (1965).
[12] G. Benedek and G. F. Nardelli, Phys. Rev. **154**, 872 (1967).

branch s. This representation is found to be particularly useful when f_{sq} displays a simple analytic behavior as a function of $\mathbf{q}$. The next section will show that only the short-range interaction is able to activate the imperfect-lattice dynamics; the long-range interaction essentially activates only the perfect-lattice dynamics.

B. Quadratic Coupling

The quadratic contribution to the surplus of perturbation on the lattice Hamiltonian is diagonal in electron quantum numbers and is of the form

$$\Lambda^{(2)}=(\pm)M_0^{-1/2}[\Phi^{(u)}-\Phi^{(g)}]M_0^{-1/2}, \tag{9}$$

where $\Phi^{(g)}$ and $\Phi^{(u)}$ are the force-constant matrices for the ground and upper states, respectively. The matrix elements of $\Lambda^{(2)}$ represent the set of coupling constants for the quadratic electron-phonon interaction. Sometimes an estimate of $\Lambda^{(2)}$ can be obtained by electrostatic arguments, considering the optically induced change of electron charge distribution. In fact in a high-symmetry center, if we assume that $\Lambda^{(2)}$ essentially receives contributions from the change of electrostatic monopole during the optic transition, we have

$$(\Phi^{(u)}-\Phi^{(g)})_{ll'}=(\beta_u-\beta_g)\frac{1}{r_0}\left(\frac{3\mathbf{x}_l\mathbf{x}_{l'}}{r_0^2}-\mathbf{1}\right)$$

if l and l' are nearest neighbors,

$$\sim 0 \quad \text{otherwise.} \tag{10}$$

β_g and β_u denote the local effective charge of the center for states g and u, respectively; r_0 is the n.n. distance, and $\mathbf{1}$ the unit dyadic. Generally, the evaluation of $\Lambda^{(2)}$ requires, however, a more sophisticated approach.

II. ABSORPTION AND EMISSION COEFFICIENTS

The absorption (emission) of light in crystals is described in terms of the distribution function $I(\Omega)$ for a specific electronic transition, $g\rightarrow u$ ($u\rightarrow g$), where Ω is the angular frequency of the electromagnetic field. To simplify matters, we assume that both u and g are nondegenerate levels. First we consider the electric-dipole transitions.

First, let us take into account only the linear and diagonal terms in electron-phonon interaction. When the thermal average is performed with the help of the usual quantum field techniques, apart from a constant factor, Eq. (1) gives

$$I(\Omega)=\frac{1}{2\pi}\int_{-\infty}^{+\infty}dt\, e^{i\Omega t}I(t), \tag{11}$$

$$I(t)=|\langle\phi_g|\mathfrak{M}|\phi_u\rangle|^2 e^{-S(T)}e^{-i\Omega_{ug}t+\varphi(T;t)}, \tag{12}$$

where, in standard notation,

$$S(T)=\tfrac{1}{2}\sum_\lambda|\Delta_\lambda|^2\coth\frac{\hbar\omega_\lambda}{2K_BT} \tag{13}$$

is the Huang-Rhys parameter, and

$$\varphi(T;t)=\tfrac{1}{2}\sum_\lambda|\Delta_\lambda|^2 \times\{[n_T(\omega_\lambda)+1]e^{-i\omega_\lambda t}+n_T(\omega_\lambda)e^{i\omega_\lambda t}\} \tag{14}$$

is the phonon-structure function. It is easy to realize that $S(T)=\varphi(T;t=0)$. The Ω_{ug} is the frequency of the zero-phonon line which, in the linear interaction approximation, is equal to $\Omega_{ug}{}^0$, the frequency for the pure electronic transition from the ground (upper) state to the "displaced" upper (ground) state.[13] $\exp[\varphi(T;t)]$ is the so-called form factor of the absorption (emission) band. $n_T(\omega_\lambda)=[\exp(\hbar\omega_\lambda/K_BT)-1]^{-1}$ is the equilibrium occupation number for phonons of type λ at absolute temperature T, K_B is the Boltzmann constant. Δ_λ is the dimensionless normal-mode "displacement" associated with the "displaced-oscillator" transformation which relates, in linear-coupling approximation, the phonons of the initial electron state to the phonons of final state.

Δ_λ is related by

$$\Delta_\lambda=\sum_{l\kappa}(\hbar\omega_\lambda{}^3M_{l\kappa})^{-1/2}\psi_\lambda(l\kappa)\cdot\mathbf{f}_{l\kappa} =(\hbar\omega_\lambda{}^3)^{-1/2}(\psi_\lambda|M^{-1/2}f) \tag{15}$$

to the force $\mathbf{f}_{l\kappa}$ that the $(l\kappa)$ ion feels immediately after the optic transition, where $\psi_\lambda(l,\kappa)$ denotes the λth normal mode. $M_{l\kappa}$ is the mass of the $(l\kappa)$ ion in the imperfect crystal (M in matrix notation). The factor $(\hbar\omega_\lambda{}^3M_{l\kappa})^{-1/2}$ has the following origin: A factor $(\hbar\omega_\lambda)^{-1}$ comes from the usual relationship between forces and relaxation (or "displacement") field, while a factor $(M_{l\kappa}\omega_\lambda/\hbar)^{-1/2}$ comes from the lattice-displacement–phonon transformation of variables. In writing Eq. (12), we have omitted the constant term that appears in Eq. (1). With this normalization, the oscillator strength $\mathfrak{f}=\int_{-\infty}^{\infty}I(\Omega)d\Omega$ of the band as a whole equals $|\langle\phi_g|\mathfrak{M}|\phi_u\rangle|^2$ whatever be the strength of the electron-phonon interaction.

Equations (12), (13), and (14) correspond to the Condon approximation. If we consider $I(t)$ beyond the Condon approximation, we cannot bring $|\langle\phi_g|\mathfrak{M}|\phi_u\rangle|$ out from the thermal average in Eq. (1) and we have to replace it by a series in powers of phonon variables. This gives rise to the electric-dipole phonon forced transitions (see Sec. IV).

[13] Notice that some authors include the strain-energy term (i.e., $\sum_\lambda\hbar\omega_\lambda|\Delta_\lambda|^2$, in harmonic approximation) in the definition of Ω_{ug}. The same term, with opposite sign, would thus appear explicitly in $\varphi(t)$ as the coefficient of a linear term in t. In writing the above expressions, we have taken into account the cancellation of these two terms. The cancellation holds also if the anharmonicity of the lattice is considered.

In terms of our coupling constants, at zero temperature, $\varphi(0;t)$ can be written as

$$\varphi(0;t)=(1/\hbar)\int_0^\infty d\omega\,\omega^{-2}e^{-i\omega t}\times\{f|\delta[\omega^2-(L_0+\Lambda(\omega^2))]|f\}\,. \quad (16)$$

We simply denote by $|f)$ the mass-normalized force vector. Hereafter, the mass-normalization will be understood: by $(l_K|f)$ we denote $M_\kappa^{-1/2}\mathbf{f}_{l_K}$. We stress that $\Lambda(\omega^2)$ in Eq. (16) denotes the lattice-dynamics perturbation for the initial electronic state.

Let us extend Eq. (16) to the case of finite temperature. Making use of (8) and (A8) we obtain

$$\varphi(T;t)=(1/\hbar)\sum_\alpha\sum_{jj'}f_{I\alpha j}f_{I\alpha j'}\int_0^\infty d\omega\times\omega^{-2}[(n_T(\omega)+1)e^{-i\omega t}+n_T(\omega)e^{i\omega t}]\rho_{I\alpha jj'}(\omega^2) \quad (17)$$

for short-range interaction, and essentially

$$\varphi(T;t)\cong\varphi_0(T;t)=(1/\hbar)\sum_s\int_0^\infty d\omega\,\omega^{-2}\langle|f_{sq}|^2\rangle_{\omega^2(s)}\times[(n_T(\omega)+1)e^{-i\omega t}+n_T(\omega)e^{i\omega t}]\rho_s{}^0(\omega^2) \quad (18)$$

for long-range interaction.

In writing Eq. (18) we have neglected the term which twice involves the joint Green-function matrix $\mathcal{G}_{\mathrm{I,II}}{}^0(z)$ (see Appendix). As $\mathcal{G}_{\mathrm{I,II}}{}^0(z)$ usually turns out to be much smaller than $\mathcal{G}_{\mathrm{I}}{}^0(z)$, this seems to be a fairly good approximation. We have further denoted by $\rho_s{}^0(\omega^2)$ the s-branch spectral density of the perfect lattice and by $\langle|f_{sq}|^2\rangle_{\omega^2(s)}$ the s branch average of f_{sq} on the constant squared-frequency surface. Hereafter we drop label I on both $\rho(\omega)$ and f: it will be restored only when its absence could generate misunderstanding. Eqs. (17) and (18) represent the starting point of our analysis. They explicitly exhibit the essential quantities which characterize the phonon process involved in the optic transition: the mass-normalized forces $f_{\alpha j}$ represent the coupling constants, while $\rho_{\alpha jj'}(\omega^2)$ $[\rho_s{}^0(\omega^2)]$ accounts for all the effects coming from the imperfect (perfect) lattice dynamics. The $f_{\alpha j}$ enter $\varphi(T;t)$ as constant factors for all the type j symmetry phonons; they *do not* depend on the lattice dynamics, and are simply related to the properties of the electron wave functions involved in the optic transitions; the only exception is represented by (18), where the forces depend, in principle, on the wave vector and the polarization of the lattice waves. The factor ω^{-2} gives the weight by which the squares of the coupling constants are shared among the perturbed (unperturbed) phonons. Notice that the electron-phonon coupling per unit frequency range is $f_{\alpha j}/\omega^{3/2}$; nevertheless a factor ω^{-2} instead of ω^{-3} appears in both expressions (17) and (18), since we are dealing with the projected density of states for the squared frequency.

When we are concerned with both linear and quadratic terms of the electron-phonon interaction we split Ω_{ug} in (12) as

$$\Omega_{ug}=\Omega_{ug}{}^0+\Delta\Omega^{(2)}\,, \quad (19)$$

where $\hbar\Omega_{ug}{}^0$ is the pure electronic transition energy and $\hbar\Delta\Omega^{(2)}$ is a self-energy correction of the upper-state (ground-state) electronic energy, given by

$$\Delta\Omega^{(2)}=-\frac{1}{4}\int_0^\infty d\omega\,\mathrm{Tr}\{\Lambda^{(2)}\rho(\omega^2)\}\coth\frac{\hbar\omega}{2K_BT}\,. \quad (20)$$

Analogously, $\varphi(T;t)$ splits as

$$\varphi(T;t)=\varphi^{(1)}(T;t)+\varphi^{(2)}(T;t)\,, \quad (21)$$

where $\varphi^{(1)}(T;t)$ is given by Eqs. (17) or (18), while $\varphi^{(2)}(T;t)$ accounts for the effect of the quadratic interaction. Starting from $\varphi^{(2)}(T;t)$ as given in the literature,[14] we rewrite it in the more explicit form

$$\varphi^{(2)}(T;t)=\frac{1}{32}\int_{-\infty}^\infty d\omega\int_0^\infty d\omega'\Bigg[\left(\frac{e^{-i\omega t}-1}{\omega^2}\right)\left(\coth\frac{\hbar(\omega-\omega')}{2K_BT}+1\right)\left(\coth\frac{\hbar\omega'}{2K_BT}+1\right)+\left(\frac{e^{i\omega t}-1}{\omega^2}\right)\left(\coth\frac{\hbar(\omega-\omega')}{2K_BT}-1\right)\left(\coth\frac{\hbar\omega'}{2K_BT}-1\right)+\frac{2it}{\omega}\left(\coth\frac{\hbar(\omega-\omega')}{2K_BT}+\coth\frac{\hbar\omega'}{2K_BT}\right)\Bigg]\theta(\omega-\omega')\times\mathrm{Tr}\{\Lambda^{(2)}\rho((\omega-\omega')^2)\Lambda^{(2)}\rho(\omega'^2)\}+\frac{1}{16}\int_{-\infty}^\infty d\omega\int_0^\infty d\omega'\Bigg[\left(\frac{e^{-i\omega t}-1}{\omega^2}\right)\left(\coth\frac{\hbar(\omega+\omega')}{2K_BT}+1\right)\left(\coth\frac{\hbar\omega'}{2K_BT}-1\right)+\frac{it}{\omega}\left(\coth\frac{\hbar(\omega+\omega')}{2K_BT}-\coth\frac{\hbar\omega'}{2K_BT}\right)\Bigg]\theta(\omega-\omega')\mathrm{Tr}\{\Lambda^{(2)}\rho((\omega+\omega')^2)\Lambda^{(2)}\rho(\omega'^2)\}\,, \quad (22)$$

[14] M. A. Krivoglatz, Fiz. Tverd. Tela **6**, 1707 (1964) [English transl.: Soviet Phys.—Solid State **6**, 1340 (1964)]; A. A. Maradudin, in *Solid State Physics*, edited by F. Seitz and D. Turnbull (Academic Press Inc., New York, 1966), Vol. 18, p. 399.

where we have also dropped the indices α, j, and j' in $\rho(\omega^2)$.

The trace on the right-hand side of Eq. (22) has the following meaning:

$$\mathrm{Tr}\{\cdots\}=\sum_\alpha d_\alpha \sum_{j_1j_2j_3j_4}\Lambda_{\alpha j_1 j_2}{}^{(2)}\rho_{\alpha j_2 j_3}(\omega^2) \times\Lambda^{(2)}{}_{\alpha j_3 j_4}\rho_{\alpha j_4 j_1}((\omega\pm\omega')^2),$$

where d_α is the dimension of the αth irr. rep. Notice that $\rho(\omega^2)$ still involves the initial-state perturbation $\Lambda(\omega^2)$.

As it stands, $\varphi^{(2)}(T;t)$ does not contribute to the first moment (i.e., peak position $\bar{\Omega}$) of the absorption (emission) band; it contributes only to the second moment (i.e., to the half width).

Moreover, it is possible to work out, from $\varphi^{(2)}(T;t)$, the quadratic contribution to the Huang-Rhys parameter and a time-dependent term which generally may produce structure. We note that the integrand on the right-hand side of Eq. (22) does not contribute to these terms as $\omega\to 0$, but is responsible for the Lorentzian shape of the zero-phonon line. Then a two-phonon structure is to be expected in principle; because of the selection rule, in high-symmetry centers this structure may essentially differ from the two-phonon structure produced by the linear interaction. Even though it is expected to be very weak, the structure produced by the quadratic interaction may be detected when local or pseudolocal phonons occur.[15]

Since greater stress is given to the effects of the linear electron-phonon interaction, in what follows $\varphi(T;t)$ means $\varphi^{(1)}(T;t)$ unless otherwise stipulated.

A. Many-Phonon Process

We consider $I(\Omega)$ in the case of short- and long-range interactions. For simplicity, we assume $T\simeq 0$°K.

i. Short-Range Interaction

a. Presence of local and pseudolocal modes. If we extract from the projected density of states the contribution coming from localized and pseudolocalized phonons [see Eqs. (A13) and (A14) in the Appendix], the form factor factorizes as

$$\exp\varphi(0;t)=\exp[\varphi_R(0;t)]\exp[\varphi_c(0;t)], \quad (23)$$

where

$$\varphi_R(0;t)=(1/\hbar)\sum_{\alpha R}|f_{\alpha R}|^2\int_0^\infty d\omega\,\omega^{-2}e^{-i\omega t}\rho_\alpha{}^R(\omega^2) \quad (24)$$

and

$$\varphi_c(0;t)=(1/\hbar)\sum_\alpha\sum_{jj'}f_{\alpha j}f_{\alpha j'}\int_0^\infty d\omega \times\omega^{-2}e^{-i\omega t}\rho_{\alpha jj'}{}^c(\omega^2). \quad (25)$$

We call $\exp\varphi_c(0;t)$ the "continuum" form factor.

If we choose the symmetry vectors $|\alpha j)$ oriented in the same direction as the R local and pseudolocal modes of symmetry α, and we keep in mind Eqs. (15) and (A14), we can write (24) as follows:

$$\varphi_R(0;t)=\tfrac{1}{2}\sum_{\alpha R}|\Delta_{\alpha R}|^2e^{-i\omega_{\alpha R}t}, \quad (26)$$

where

$$|\Delta_{\alpha R}|^2=(1/\hbar)|f_{\alpha R}|^2\omega_{\alpha R}{}^{-3} \times\frac{1}{|\Lambda_{\alpha R}(\omega^2{}_{\alpha R})\,\mathrm{Re}\mu_{\alpha R}{}'(\omega^2{}_{\alpha R})|}. \quad (27)$$

Equation (27) gives the relation between the local- or pseudolocal-normal mode displacement $\Delta_{\alpha R}$ and the projection of the mass normalized force $f_{\alpha R}$ on the oriented symmetry vector $|\alpha R)=|v_{\alpha R})$ (see Appendix). $\exp\varphi_R(0;t)$ can be Taylor-expanded with respect to $\varphi_R(0;t)$ and the terms in the resulting series rearranged in powers of $\exp(-i\omega_{\alpha R}t)$. Thus, $I(t)$ turns out to be an infinite series of terms involving the product of exponentials of the type $\exp(-i\omega_{\alpha R}t)$ multiplied by the continuum form factor. Let $I_{n_{\alpha'R'},n_{\alpha''R''},\ldots}{}^{(n)}(\Omega)$ denote the "n-phonon term" in the distribution function $I(\Omega)$, i.e., the contribution to $I(\Omega)$ coming from the Fourier-transform of the term in $I(t)$ which involves $n_{\alpha'R'}$ local or pseudolocal phonons of frequency $\omega_{\alpha'R'}$, $n_{\alpha''R''}$ local or pseudolocal phonons of frequency $\omega_{\alpha''R''}$ and so on, for a total of $n=n_{\alpha'R'}+n_{\alpha''R''}+\cdots$ local or pseudolocal phonons. Then we have

$$I(\Omega)=\sum_n\sum_{\{n_{\alpha R}\}}I_{n_{\alpha'R'},n_{\alpha''R''},\ldots}{}^{(n)}(\Omega),$$

where

$$I_{n_{\alpha'R'},n_{\alpha''R''},\ldots}(\Omega)=(\tfrac{1}{2}|\Delta_{\alpha'R'}|^2)^{n_{\alpha'R'}}/(n_{\alpha'R'})!\times(\tfrac{1}{2}|\Delta_{\alpha''R''}|^2)^{n_{\alpha''R''}}/(n_{\alpha''R''})!\cdots\times I_c(\Omega-n_{\alpha'R'}\omega_{\alpha'R'}-n_{\alpha''R''}\omega_{\alpha''R''}-\cdots). \quad (28)$$

$I_c(\Omega)$ is found to have the following expression:

$$I_c(\Omega)=|\langle\mathfrak{M}\rangle|^2\exp[-S(0)]\int_{-\infty}^{+\infty}dt \times\exp[it(\Omega-\Omega_{ug})+\varphi_c(0;t)]. \quad (29)$$

We call Eq. (28) the "generating function" for the absorption (emission) band in presence of local and pseudolocal modes. Apart from a numerical factor, it appears that every n-phonon term $I_{n_{\alpha'R'},n_{\alpha''R''},\ldots}{}^{(n)}(\Omega')$ reproduces, at the combined frequency

$$\Omega'=\Omega-(n_{\alpha'R'}\omega_{\alpha'R'}+n_{\alpha''R''}\omega_{\alpha''R''}+\cdots), \quad (30)$$

the distribution function $I_c(\Omega)$ for the continuum-phonon process. We emphasize that here we call the "n-phonon term" a term which, in the rearranged Taylor expansion of the form factor, involves n local and pseudolocal phonons, variously combined, and an arbitrarily large number of continuum phonons.

As $\varphi_c(0;t)$ in (25) is a normalizable generalized function well-behaved at infinity,[16] $I_c(\Omega)$ displays at $\Omega=\Omega_{ug}$

[15] D. G. Thomas, J. Phys. Soc. Japan Suppl. 21, 270 (1966).

[16] M. J. Lighthill, in *Fourier Analysis and Generalized Functions* (Cambridge University Press, Cambridge, England, 1963).

a rather sharp δ-type line that is well resolved from the smooth sideband which may be present at higher (lower) frequencies. The lower the density $\rho_\alpha{}^c(\omega^2)$ of continuum phonons allowed in the optic transition, the more intense is the δ-type line of $I_c(\Omega)$, in comparison with the sideband. From Eq. (28) it follows that the so-called multiple-phonon lines in the whole band are nothing but a repetition of the δ-type line of $I_c(\Omega)$.

Split the Huang-Rhys parameter as

$$S(0)=S_R(0)+S_c(0)=\sum_{\alpha R} S_{\alpha R}(0)+S_c(0), \quad (31)$$

where $S_c(0)$ represents the continuum-phonon contribution. The zero-temperature oscillator strength $\mathfrak{f}_c(0)$ associated with $I_c(\Omega)$ is

$$\mathfrak{f}_c(0)=|\langle \mathfrak{M}\rangle|^2 \exp[-S_R(0)], \quad (32)$$

whereas the oscillator strength of the δ-type line is

$$\mathfrak{f}^{(0)}(0)=|\langle \mathfrak{M}\rangle|^2 \exp[-S(0)]. \quad (33)$$

Therefore

$$\exp[-S_c(0)]=\mathfrak{f}^{(0)}(0)/\mathfrak{f}_c(0) \quad (34)$$

gives the fractional intensity of the δ-type line in $I_c(\Omega)$.

With reference to Eq. (28), the oscillator strength associated with the whole band can be further split as

$$|\langle \mathfrak{M}\rangle|^2=\mathfrak{f}^{(\mathrm{m.p.h.})}(0)+\mathfrak{f}^{(\mathrm{B.ab.})}(0),$$

where

$$\mathfrak{f}^{(\mathrm{m.ph.})}(0)=|\langle \mathfrak{M}\rangle|^2 \exp[-S_c(0)],$$
$$\mathfrak{f}^{(\mathrm{B.ab.})}(0)=|\langle \mathfrak{M}\rangle|^2\{1-\exp[-S_c(0)]\},$$

and, therefore,

$$\mathfrak{f}^{(\mathrm{m.ph.})}(0)/\mathfrak{f}^{(\mathrm{B.ab.})}(0)=1/\{\exp[S_c(0)]-1\}. \quad (35)$$

$\mathfrak{f}^{(\mathrm{m.ph.})}(0)$ is the oscillator strength associated with all the multiple-phonon lines in $I(\Omega)$, while $\mathfrak{f}^{(\mathrm{B.ab.})}(0)$ is the oscillator strength for the background absorption (emission) in the whole band. $S_c(0)$ can be easily evaluated with the help of Eqs. (A13) and (A14). Eq. (35) tells us how the total intensity of the band is shared among multiple-phonon lines and broad background absorption. The oscillator-strength ratio of two subsequent multiple-phonon lines is given by

$$\mathfrak{f}^{(n_{\alpha R}+1)}(0)/\mathfrak{f}^{(n_{\alpha R})}(0)=\tfrac{1}{2}|\Delta_{\alpha R}|^2/(n_{\alpha R}+1). \quad (36a)$$

We observe from Eq. (13) that $S_{\alpha R}(0)=\frac{1}{2}|\Delta_{\alpha R}|^2$, so Eq. (36a) may also be written as

$$\mathfrak{f}^{(n_{\alpha R}+1)}(0)/\mathfrak{f}^{(n_{\alpha R})}(0)=S_{\alpha R}(0)/(n_{\alpha R}+1). \quad (36b)$$

Equations (36) represent the "intensity law" of the multiple-phonon lines at $T=0°\mathrm{K}$.

At finite temperature, the intensity laws (33) and (36b) may be obtained with a procedure similar to that used in connection with the Mössbauer effect.[3] They take the following forms:

$$\mathfrak{f}^{(0)}(T)/\mathfrak{f}=e^{-S(T)}\mathrm{I}_0((x_c y_c)^{1/2})\Pi_{\alpha R}\mathrm{I}_0((x_{\alpha R}y_{\alpha R})^{1/2}) \quad (33')$$

and

$$\mathfrak{f}^{(n_{\alpha R}+1)}(T)/\mathfrak{f}^{(n_{\alpha R})}(T)$$
$$=(x_{\alpha R}y_{\alpha R})^{-1/2}\frac{(x_{\alpha R}{}^{n_{\alpha R}+1}+y_{\alpha R}{}^{n_{\alpha R}+1})}{(x_{\alpha R}{}^{n_{\alpha R}}+y_{\alpha R}{}^{n_{\alpha R}})}$$
$$\times\frac{I_{n_{\alpha R}+1}((x_{\alpha R}y_{\alpha R})^{1/2})}{I_{n_{\alpha R}}((x_{\alpha R}y_{\alpha R})^{1/2})}, \quad (36c)$$

where $I_n((x_iy_i)^{1/2})$ is the modified Bessel function of nth order of the argument $x_i=S_i(T)-S_i(0)$ times $y_i=S_i(T)+S_i(0)$, $(i=c,\alpha R)$.

Concerning the symmetry α of the phonons involved in the optic transition, the linear interaction selection rule is

$$\alpha \in [\alpha_u\otimes\alpha_u]+[\alpha_g\otimes\alpha_g], \quad (37)$$

where α_g and α_u are the irr. reps. according to which the ground- and upper-electronic states transform, respectively. $[\cdots\otimes\cdots]$ denotes symmetric product. If the point group contains the inversion operation, α must have even parity. This, for cubic point groups, means that phonons which transform according to T_{1u} (the infrared active) irr. rep. cannot be involved in dipole-allowed optic transitions; only the phonons which transform according to even irr. reps. such as A_{1g} ("breathing" mode), E_g and T_{2g} can be involved. The richer the point group in symmetry operations, the better the selection rule (37) operates. As a consequence of Eq. (37), the absorption (emission) band can display multiple-phonon lines only when the local and pseudo-local modes fall into the allowed symmetries.

b. Absence of local and pseudolocal modes. The many-phonon process involves continuum phonons only. Then $I(\Omega)$ has formally the same form as $I_c(\Omega)$ Eq. (29), in which $\varphi_c(0;t)$ is now replaced by the whole $\varphi(0;t)$. Of course, only the zero-phonon line occurs: $\exp[-S(0)]$ gives its fractional intensity [see (34)]. $\varphi(0,t)$ usually retains some more memory of the peaks which occur in the phonon spectral density than $\varphi_c(0;t)$, memory which is reflected in the absorption (emission) band by the appearance of a more pronounced continuum-phonon vibrational structure. The main peaks are, however, expected in the region of the one-phonon frequencies.

ii. Long-Range Interaction

In dealing with optic transitions, the most typical long-range interaction corresponds to the force field of an electric dipole. When neither quadrupole nor appreciable exchange occurs, the electron-phonon interaction is dominated by the long-range part of the dipole field, and with good approximation we can use Eq. (18) for $\varphi(0;t)$. In such a case, the distribution

function reads

$$I(\Omega)\simeq|\langle\mathfrak{M}\rangle|^2\exp[-S(0)]\int_{-\infty}^{+\infty}dt \times\exp[i(\Omega-\Omega_{ug})t+\varphi_0(0;t)] \quad (38)$$

independently of the existence of local or pseudolocal modes. $\varphi_0(0;t)$ involves the unperturbed density of states; the possible peaks of $I(\Omega)$ are then to be assigned to the unperturbed phonons of the host lattice.

We note that $\exp[\varphi_0(0;t)]$ in (38), as well as $\exp[\varphi_c(0;t)]$ in (29), in the presence of local and pseudolocal modes, or $\exp[\varphi(0;t)]$ in (12), in the absence of local or pseudolocal modes, always generate a many-phonon process which involves the continuum phonons only. Either the perturbed or the essentially unperturbed continuum phonons enter the description of such a process, depending upon whether the electron-phonon interaction is dominated by short- or long-range interaction.

B. Continuum-Phonon Process

We give here some more details about $I_c(\Omega)$. We have to replace $\rho_\alpha{}^c(\omega^2)$ in (25) by $\rho_\alpha(\omega^2)$, when no local (pseudolocal) modes occur, or by $\rho_s{}^0(\omega^2)$ when dipolar forces dominate the electron-phonon interaction; when this is done, the following discussion will apply equally well, to these cases.

Because of the continuum character of the wavelike modes, every n-phonon term of a Taylor expansion of the continuum form factor will be a convolution of n projected densities, so that the shape of the n-phonon term is not related in a simple way to that of the preceeding terms. This explains why no repeated structures occur in $I_c(\Omega)$, and why $I_c(\Omega)$ has been kept apart in writing (28).

We keep the zero-phonon line at $\Omega=\Omega_{ug}$ out of $I_c(\Omega)$ and we analyze the possible discontinuities of the remaining expressions by the method of the asymptotic developments. We assume, for simplicity, that every irr. rep. appears singly in (25).

Because of the existence of critical points in the Brillouin zone,[17] $\rho_\alpha{}^c(\omega^2)$ is not smooth, but is a function in the generalized sense.[16,18] Elsewhere, two of us[19] have discussed what kind of discontinuities can occur in $\rho_\alpha{}^c(\omega^2)$. These discontinuities occur at the frequencies $\omega_{c,i}$ of the critical points in the unperturbed density of states, and involve essentially the first- and second-order derivatives of $\rho_\alpha{}^c(\omega^2)$. As a consequence, $I_c(\Omega)$ also has

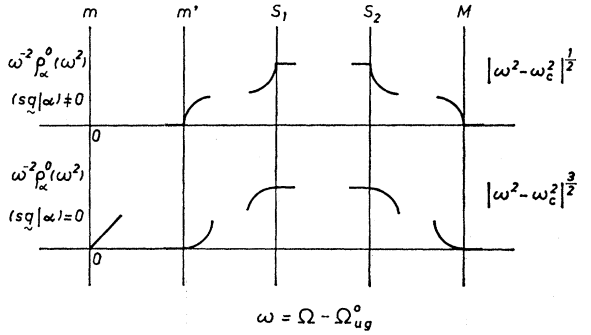

FIG. 1. Analytic critical points of $\omega^{-2}\rho_\alpha{}^0(\omega^2)$ versus ω: (a) when $(s\mathbf{q}|\alpha)\neq 0$, and (b) when $(s\mathbf{q}|\alpha)=0$. m and m' denote absolute and relative minima, respectively.

discontinuities and these are wholly specified by the asymptotic behavior of $\exp[\varphi_c(0;t)]$ (or $\exp[\varphi_0(0;t)]$).

If M denotes the total number of critical points in the Brillouin zone, $\varphi_c(0;t)$ can be written as

$$\varphi_c(0;t)=(1/\hbar)\sum_\alpha|f_\alpha|^2\sum_{i=1}^{M}\int_0^\infty d\omega\,\omega^{-2}e^{-i\omega t}\rho_\alpha{}^c(\omega^2) \times\theta(\omega_{c,i}-\omega)\theta(\omega-\omega_{c,i-1}), \quad (39)$$

where $\theta(\omega)$ is the Heaviside step function. Lighthill's tables[16] tell us that, for analytic critical points, every term of (39) behaves asymptotically either as $t^{-3/2}\exp[-i\omega_{c,i}t]$ or $t^{-5/2}\exp[-i\omega_{c,i}t]$, depending upon whether $(\alpha|\mathbf{q}_{c,i},s)\neq 0$ or $(\alpha|\mathbf{q}_{c,i},s)=0$. $\mathbf{q}_{c,i}$ is the critical point wave vector in the Brillouin zone. Negative powers of a higher order occur if nonanalytic critical points are present. By expanding $\exp[\varphi_c(0;t)]-1$ in powers of $\varphi_c(0;t)$, one recognizes that the lowest-order discontinuities that can appear in $I_c(\Omega)$ are those shown in Figs. 1 and 2, respectively. These types of discontinuities come essentially from the one-phonon process.

It is worth noticing that peaks and critical points of $\rho_\alpha{}^c(\omega^2)$ [or $\rho_s{}^0(\omega^2)$] do not occur at the same frequency and apparently are not closely related to one another. We emphasize that the most markedly vibrational structure in $I_c(\Omega)$ comes from the possible peaks of $\rho_\alpha{}^c(\omega^2)$ rather than from the critical points. When one or more well-pronounced local (pseudolocal) modes occur, $\rho_\alpha(\omega^2)$ is, however, dominated by the local (pseudolocal) mode contribution. In this case and within experimental accuracy, the Fourier transform of $\exp[\varphi_c(0;t)-1]$ is expected to behave as a smooth function.

As regards the discontinuities due to the quadratic interaction, we have studied the critical points of the two-phonon density of states. The frequency at which such points are expected is the sum or the difference of two critical-point frequencies of the one-phonon projected density of appropriate symmetry. It is not worthwhile to enter into further details, because the

[17] L. Van Hove, Phys. Rev. **89**, 1189 (1953); J. C. Phillips, *ibid.* **104**, 1293 (1956).

[18] A. A. Maradudin and J. Peretti, Comp. Rend. **247**, 2310 (1958).

[19] E. Mulazzi and N. Terzi, in *Proceedings of the Conference on Electronic and Ionic Properties of Alkali Halides*, edited by R. Fieschi and G. Spinolo (Gruppo Nazionale di Struttura della Materia, Istituto di Fisica dell'Università, Milan, Italy, 1966). See also Y. Toyozawa, M. Inoue, T. Inui, M. Okazaki, and E. Hanamura, J. Phys. Soc. Japan **21**, Suppl. 133 (1966).

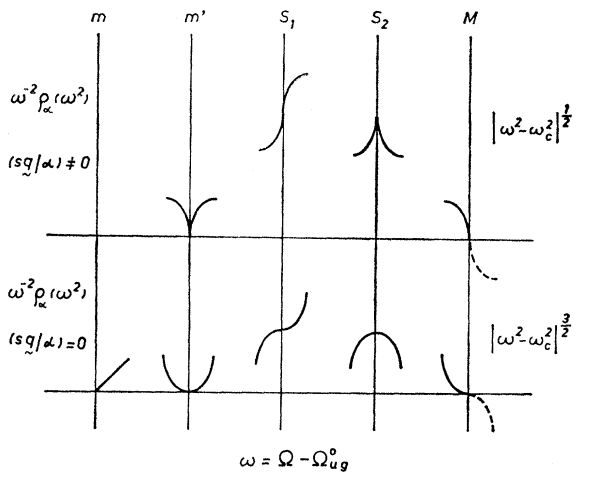

FIG. 2. Analytic critical points of $\omega^{-2}\rho_\alpha(\omega^2)$ versus ω: (a) when $(sq|\alpha)\neq 0$, and (b) when $(sq|\alpha)=0$. m and m' denote absolute and relative minima, respectively.

intensity of this structure is expected to be very weak. We only mention that the behavior of the analytical critical points of the unperturbed two-phonon projected density of states is very similar to that shown in Figs. 1(a), 1(b), 2(a), and 2(b).

From the behavior of the integrand in Eq. (39) in the low-frequency region, it is possible to give some predictions of the shape of the band near Ω_{ug}, the zero-phonon-line frequency. For high-symmetry centers and short-range interactions, $\rho_{\alpha jj'}(\omega^2)$ behaves as ω^3 near $\omega=0$ because $(s,\mathbf{q}=0|\alpha_j)=0$. Because of the factor ω^{-2}, which appears in the integrand (39), the sideband of the zero-phonon line is expected to start from Ω_{ug} with a linear behavior. For low-symmetry centers and for a dipole field of force, it is instead $(f|\delta(\omega^2-L)|f)\omega^{-2}$ that behaves as ω^3 near $\omega=0$. Thus the sideband of the zero-phonon line is, in such a case, expected to start from Ω_{ug} with an ω^3 behavior.[9]

III. CONFIGURATION-DIAGRAM DESCRIPTION

The starting point of the configuration-diagram description is the analysis of the way the energy $\Delta\Omega^{(1)}$, which the many-phonon process contributes to the pure electronic energy $\hbar\Omega_{ug}$, on the average, is distributed in frequency.[20–24,4] We show that as long as $S\gg 1$ (we are concerned only with peak frequency $\bar{\Omega}$ and half-width H of the band), the exact expression for $I(\Omega)$ is reasonably consistent with a configuration-diagram description. However, particular care must be taken in dealing with this diagram when local or pseudolocal modes occur.

Let us assume, first, that no local (pseudolocal) modes with appropriate symmetry occur. In such a case, $\varphi(t)$ is well behaved to infinity, i.e., it does not display any oscillating term as $t\to\pm\infty$ and goes to zero faster than t^{-1}. Furthermore, at short times, it is expected to display an oscillatory behavior with a maximum amplitude at $t=0$, where $\varphi(0)=S$. When S is much higher than unity, $\mathrm{Re}[\varphi(t)-S]$ reaches large negative values, quite rapidly as t increases from 0.

The short-time approximation can then be employed for $I(t)$. We have

$$\exp[-S+\varphi(t)]\cong\exp\left[-i\Delta\Omega^{(1)}t-\frac{H^2t^2}{8\ln 2}\right]. \quad (40)$$

Fourier inversion then leads straightforwardly to

$$I(\Omega)\cong|\langle\mathfrak{M}\rangle|^2(1/(2\pi)^{1/2}\sigma)\exp[-\tfrac{1}{2}(\Omega-\bar{\Omega})^2/\sigma^2] \quad (41)$$

with peak frequency

$$\bar{\Omega}=\Omega_{ug}+\Delta\Omega^{(1)}, \quad (42)$$

$$\Delta\Omega^{(1)}=(1/\hbar)\sum_\alpha\sum_{jj'}\bar{f}_{\alpha j}\bar{f}_{\alpha j'}\int_0^\infty d\omega\,\omega^{-1}\rho_{\alpha jj'}(\omega^2), \quad (43)$$

and half-width $H=(8\ln 2)^{1/2}\sigma$ given at $T=0°\mathrm{K}$ by

$$H^2=(8\ln 2)(1/\hbar)\sum_\alpha\sum_{jj'}\bar{f}_{\alpha j}\bar{f}_{\alpha j'}\int_0^\infty d\omega\,\rho_{\alpha jj'}(\omega^2). \quad (44)$$

This is just the Gaussian approximation. In the above expression, we have put [see Eq. (A5)]

$$\rho_{\alpha jj'}(\omega^2)=(j\alpha|\,\delta(\omega^2-L)\,|\alpha j')$$
$$=\sum_{mm'}(j\alpha|\,(M/M_0)^{1/2}|\alpha m)\rho_{\alpha mm'}(\omega^2)\times(m'\alpha|\,(M/M_0)^{1/2}|\alpha j'),$$

where $\rho_{\alpha mm'}(\omega^2)$ denotes the projected density with the old normalization [see Eq. (A17)]. The normalization of $\rho_{\alpha jj'}(\omega^2)$ is simply $\delta_{jj'}$.

Notice the new mass normalization of the forces, i.e., $\bar{f}_{\alpha j}\equiv(j\alpha|M^{-1/2}M_0^{1/2}f)$, where f is the force with the old normalization. By defining the weight function

$$2\omega\rho_\alpha'(\omega^2)=2\omega\sum_{jj'}\rho_{\alpha jj'}(\omega^2),$$

$$\int_0^\infty d\omega\,2\omega\rho_\alpha'(\omega^2)=n_\alpha d_\alpha, \quad (45)$$

where n_α is the number of times the αth irr. rep. occurs in the coefficients (i.e., $\bar{f}_{\alpha j}$) of the electron-phonon interaction and d_α its dimension, we find it convenient to introduce the frequency-dependent α-symmetry displacement $\Delta_\alpha(\omega)$:

$$(\Delta_\alpha(\omega))^2\equiv(1/\rho_\alpha'(\omega^2))\sum_{jj'}(\bar{f}_{\alpha j}\bar{f}_{\alpha j'}/\hbar\omega^3)\rho_{\alpha jj'}(\omega^2). \quad (46)$$

It turns out that the square of this α-symmetry displacement is distributed in frequency according to the weight

[20] D. L. Dexter, in *Solid State Physics*, edited by F. Seitz and D. Turnbull (Academic Press Inc., New York, 1958), Vol. 6, p. 353.
[21] J. J. Markham, Rev. Mod. Phys. **31**, 956 (1959).
[22] W. B. Fowler and D. L. Dexter, Phys. Rev. **128**, 2154 (1962).
[23] C. C. Klick, D. H. Patterson, and R. S. Knox, Phys. Rev. **133**, 1717 (1964).
[24] The configurational diagram is usually introduced when a local mode dominates the motion of the ions around the defects.

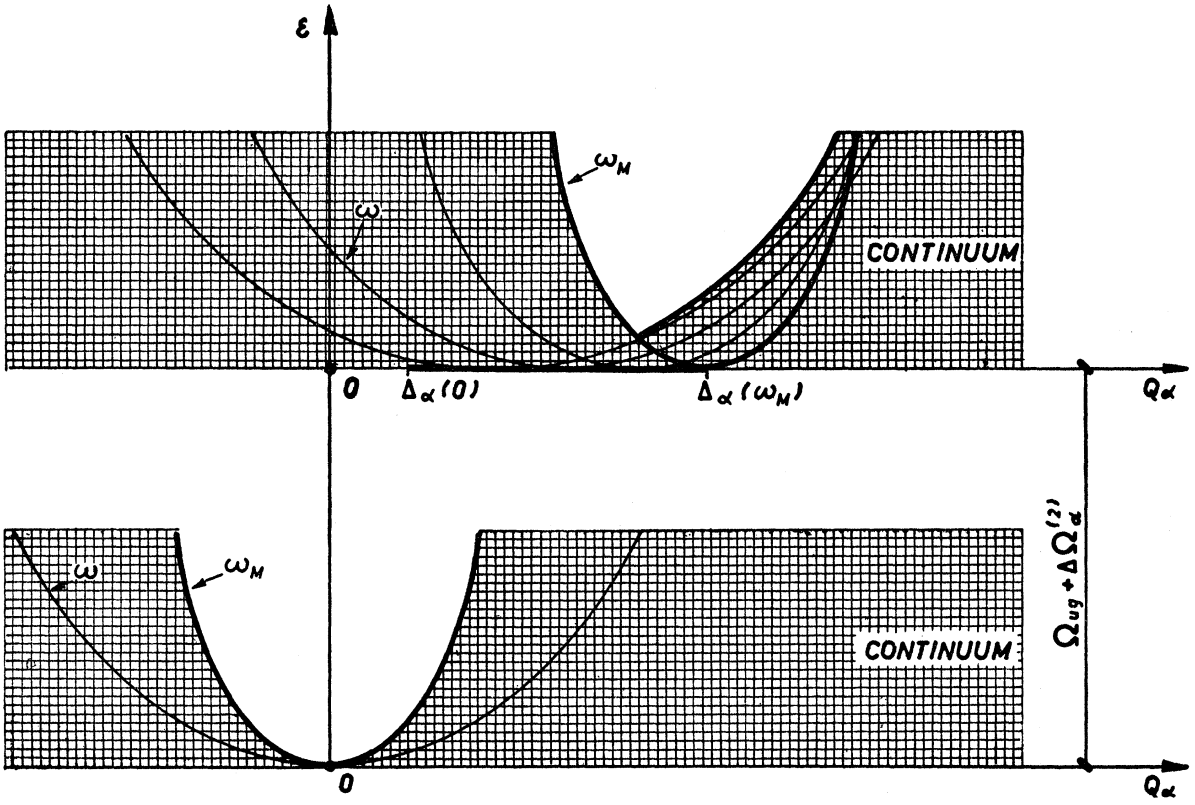

FIG. 3. Continuum of vibrational states involved in the optic transition (absorption).

function $2\omega\rho_\alpha'(\omega^2)$, with a mean value

$$\langle(\Delta_\alpha(\omega))^2\rangle_{\mathrm{av}(\rho_\alpha')} \equiv |\Delta_{\alpha,\mathrm{eff}}|^2 = 2S_\alpha(T\sim 0)$$
$$= (2/\hbar)\sum_{jj'}\int_0^\infty d\omega$$
$$\times \tilde{f}_{\alpha j}\tilde{f}_{\alpha j'}\omega^{-2}\rho_{\alpha jj'}'(\omega^2). \quad (47)$$

In view of (43) and (46), we say that the continuum phonons with symmetry α and frequency ω, on the average, give the contribution

$$\hbar\Delta\Omega_\alpha^{(1)}(\omega) = \tfrac{1}{2}\hbar\omega(\Delta_\alpha(\omega))^2 \quad (48)$$

to the energy of the optic transition, the α-symmetry phonons themselves being described in frequency according to the weight function $2\omega\rho_\alpha'(\omega^2)$. In order to find the connection with the configuration diagram, we consider the mean square displacement of the α-symmetry projected configurational coordinate Q_α. At $T=0°\mathrm{K}$

$$\langle 0||Q_{\alpha,o_p}|^2|0\rangle \equiv \sum_{jj'}\sum_\lambda (j\alpha|\psi_\lambda)\langle 0||Q_{\lambda,o_p}|^2|0\rangle(\psi_\lambda|\alpha j')$$
$$= \tfrac{1}{2}\sum_{jj'}\sum_\lambda (j\alpha|\psi_\lambda)(\psi_\lambda|\alpha j')$$
$$= \frac{1}{2}\int_0^\infty d\omega\, 2\omega\rho_\alpha'(\omega^2) = \tfrac{1}{2}n_\alpha d_\alpha, \quad (49)$$

where $|0\rangle$ denotes the vacuum-phonon state for the initial electronic level.

Keeping Eq. (45) in mind, Eq. (49) can be interpreted as though the projected mean square displacement of any of the $n_\alpha d_\alpha$ α-symmetry phonons of frequency ω were $\frac{1}{2}$. Furthermore, Eq. (48) tells us that, for every frequency ω, the energy $\hbar\Delta\Omega_\alpha^{(1)}(\omega)$ contributed by the α-symmetry phonons is just the intercept on the ordinate axis of the adiabatic energy function

$$\epsilon_u(\omega; Q_\alpha) = \hbar\Omega_{ug} + \tfrac{1}{2}\hbar\omega[Q_\alpha - \Delta_\alpha(\omega)]^2, \quad (50)$$

once the zero-phonon energy is divided out. ω plays the role of a continuous parameter. At $T=0°\mathrm{K}$ the projected configurational coordinate Q_α has a standard deviation σ_{Q_α} from $Q_\alpha=0$ equal to

$$\sigma_{Q_\alpha} = \sqrt{\tfrac{1}{2}}. \quad (51)$$

If this standard deviation is projected onto the adiabatic energy function Eq. (50) (see Figs. 3 and 4), and if afterwards the corresponding standard deviation for the energy is first squared and then averaged with the help of the weight function Eq. (45), it is easy to verify that the resulting expression gives exactly the rigorous expression Eq. (44). This is only to say that, for $S\gg 1$, the α-symmetry phonons of different frequency enter the many-phonon process as statistically independent entities. However, in order to find consistency with

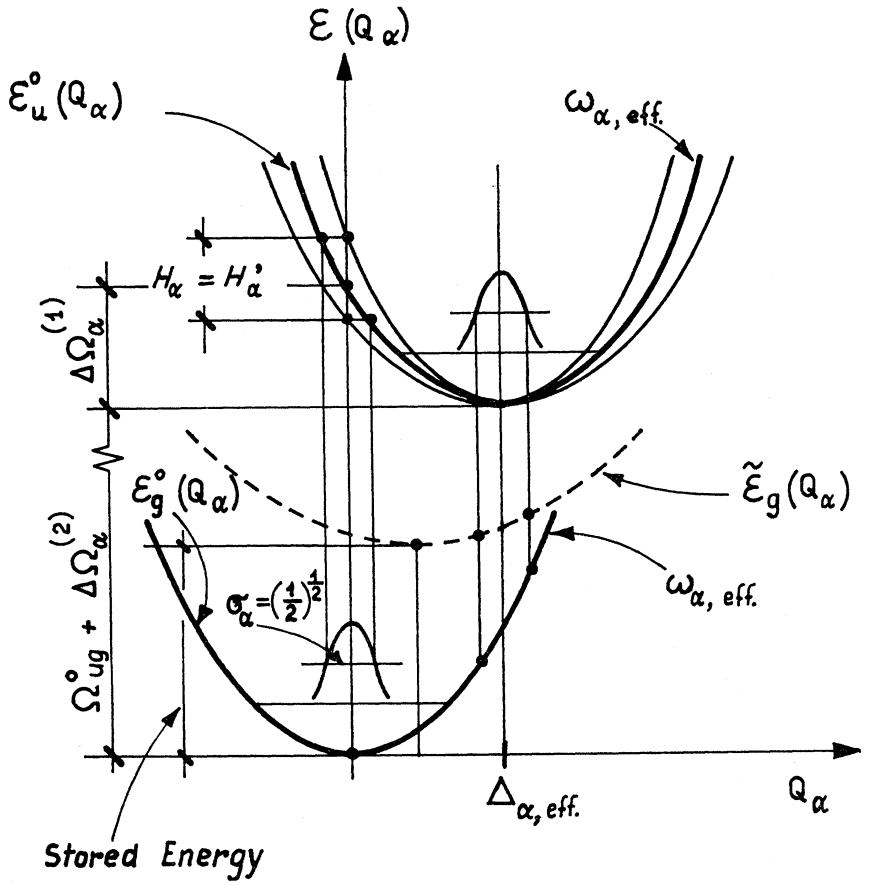

FIG. 4. Configurational diagram (absorption) in the absence of local and pseudolocal modes. $\epsilon_g^0(Q_\alpha)$ and $\epsilon_u^0(Q_\alpha)$ denote adiabatic energy functions. $\tilde{\epsilon}_g(Q_\alpha)$ denotes a hypothetic adiabatic energy function for the polarized ground state. It might occur for "intermediate bonding." The difference between the minima of $\epsilon_u^0(Q_\alpha)$ and $\tilde{\epsilon}_g(Q_\alpha)$ would appear as a stored-energy term in the Stokes shift between absorption and emission bands.

Eq. (44) we must average the square of the energy standard deviation and not the standard deviation itself. The situation is shown in Fig. 3. We have reported on the abscissa the projected configuration coordinate Q_α. A continuum of vibrational states of α symmetry exists for both electronic states g and u; they correspond to the infinite set of parabolas whose curvature ranges from $\omega=0$ to the maximum $\omega=\omega_M$. We stress that $\hbar\Omega_{ug}=\hbar(\Omega_{ug}{}^0+\Delta\Omega^{(2)})$ denotes here the energy of the zero-phonon line. The $\hbar\Omega_{ug}{}^0$ is the energy of the pure electronic transition. Let us consider the upper-state parabola, which corresponds to a given vibrational frequency ω; apart from the energy of the zero-phonon line, it crosses the ordinate axis exactly at the point $\frac{1}{2}\hbar\omega(\Delta_\alpha(\omega))^2$. We may say that the continuum-phonon process corresponds to the superposition of all the vertical transitions that start at the origin of the configurational diagram and reach every single parabola embedded in the upper-state continuum; this continuum behaves as if the parabolas were distributed according to the weight function of Eq. (45).

The zero-phonon transition enters the present description as a "tunneling" between the phonon vacuums of ground and upper state. We can explain the dispersion in frequency associated with the optic transition by the following procedure.

Define an effective vibrational frequency by

$$(\omega_{\alpha,\text{eff}})^2=\int_0^\infty \omega^2(\Delta_\alpha(\omega))^2 2\omega\rho_\alpha'(\omega^2)d\omega \Big/ \int_0^\infty (\Delta_\alpha(\omega))^2 2\omega\rho_\alpha'(\omega^2)d\omega=\langle\omega^2\rangle_{\text{av}(\Delta_\alpha{}^2\rho_{\alpha'})}. \quad (52)$$

Thus, in view of Eqs. (44) and (47), we can write $H_\alpha{}^2$ in the usual form:

$$H_\alpha{}^2=(8\ln 2)(\omega_{\alpha,\text{eff}})^2 S_\alpha(T\sim 0). \quad (53)$$

The last equality in (52) defines the average operation $\langle\cdots\rangle_{\text{av}(\Delta_\alpha{}^2\rho_{\alpha'})}$. Equation (52) gives unambiguously the wanted definition of the effective vibrational frequency. A different $\omega_{\alpha,\text{eff}}$ occurs for phonons of different symmetry. The weight function $\Delta_\alpha{}^2(\omega)\rho_\alpha'(\omega^2)$, entering the definition of $\omega_{\alpha,\text{eff}}$, represents the combined effect of the host-lattice dynamics and electron-phonon interaction. We can put the configurational diagram of Fig. 3 into a more familiar form. For the sake of simplicity, we consider a system of two nondegenerate electron levels. From the upper-state vibrational continuum of Fig. 4, we select a suitable parabola and an appropriate frequency dispersion with the purpose of simulating the α-symmetry continuum. We characterize this parabola

by the effective vibrational frequency $\omega_{\alpha,\text{eff}}$, Eq. (52), and by the effective α-symmetry displacement $\Delta_{\alpha,\text{eff}}$, Eq. (47). Analogously, the ground-state vibrational continuum of α symmetry is simulated by a single parabola starting at the origin of the configurational diagram, with the same effective frequency $\omega_{\alpha,\text{eff}}$ as that of the upper state, and without dispersion.

Usually, the frequency dispersion associated with the many-phonon process is deduced from the configuration diagram by projecting the ground-state standard deviation σ_{Q_α} of the configuration coordinate Q_α at thermal equilibrium, upon the upper-state parabola. Let H_α' be the contribution to the halfwidth of the absorption band deduced by this graphical method. An inspection of both Fig. 4 and Eqs. (50) and (51) tells us that

$$(H_\alpha')^2 \simeq \tfrac{1}{2}(8\ln 2)\langle\omega^2\rangle_{\text{av}(\Delta_\alpha{}^2\rho_{\alpha'})}\langle\Delta_\alpha{}^2\rangle_{\text{av}(\rho_{\alpha'})} = (8\ln 2)(\omega_{\alpha,\text{eff}})^2 S_\alpha(T\sim 0)\,. \tag{54}$$

We denoted by $\text{av}(\rho_\alpha')$ the averaging operation, which appears in Eq. (47). $(H_\alpha')^2$ looks the same as $H_\alpha{}^2$ [Eq. (53)]. This result is not surprising as the Gaussian approximation is equivalent to treating the many-phonon process as a classical process. In principle, we should consider a diagram for each symmetry; however, by defining

$$(\omega_{\text{eff}})^2 = \textstyle\sum_\alpha (\omega_{\alpha,\text{eff}})^2 (S_\alpha/S)\,, \qquad |\Delta_{\text{eff}}| = [2S(T\sim 0)]^{1/2}\,, \tag{55}$$

a single diagram can be employed for most practical uses.

We assume now that a α-symmetry local mode of frequency $\omega_{\alpha R}$ occurs in the imperfect-lattice dynamics. Figure 5 shows the configuration diagram for such a case. With respect to $\Delta_{\alpha,\text{eff}}$ as previously introduced, $\Delta_{\alpha R}$ retains now a microscopic meaning. This fact prevents us the use of this configuration diagram in the usual way. The $\rho_\alpha(\omega^2)$ splits into local- and continuum-mode terms $\rho_\alpha{}^R(\omega^2)$ and $\rho_\alpha{}^C(\omega^2)$, respectively. However, it may happen that the normalization of $\rho_\alpha{}^R(\omega^2)$ is very close to unity and, at the same time, the electron-phonon interaction involves essentially the α-symmetry phonons. In such a case, the distribution function $I_e(\Omega)$ for the continuum-phonon process is expected to display a fairly well resolved zero-phonon line, even when $S\gg 1$. The local modes' parabolas in Fig. 5 may then dominate the process so that the discrete nature at the quantum levels for the local mode has to be taken into consideration. Furthermore, it is not clear how to define the halfwidth of the whole band, because the band is characterized by the peaks at one, two, etc., local phonons, for which the intensity law is $e^{-S_R}(S_R)^n/n!$.

IV. ELECTRIC-DIPOLE FORCED PROCESS

As stated in Sec. I, the "nondiagonal" part of the electron-phonon interaction leads to a mixing of the electron wave functions. This is reflected in the absorption (emission) band by the electric-dipole transitions forced by phonons.

To simplify, let us assume that g is a pure (i.e., unmixed) electronic state; in the framework of the adiabatic principle, we may account for the wave-function mixing by writing the matrix element of the dipole moment as

$$\mathfrak{M}_{ug}(b_\lambda) = \mathfrak{M}_0 + \textstyle\sum_\lambda \mathfrak{M}_\lambda (b_\lambda + b_\lambda{}^+)\,, \tag{56}$$

where

$$\mathfrak{M}_0 = \mathfrak{M}_{ug}{}^0 - \textstyle\sum_\lambda \mathfrak{M}_\lambda \Delta_\lambda{}^*$$

and

$$\mathfrak{M}_\lambda = \textstyle\sum_{i\neq u} (2\hbar\omega_\lambda)^{-1/2}\left(\dfrac{\hbar}{\epsilon_u{}^0-\epsilon_i{}^0}\right)\sum_{lk} M_{lk}{}^{-1/2}\psi_\lambda{}^*(lk)\cdot \mathbf{f}_{lk}{}^{ui}\mathfrak{M}_{ig}{}^0$$
$$= \textstyle\sum_{i\neq u} (2\hbar\omega_\lambda)^{-1/2}\left(\dfrac{\hbar}{\epsilon_u{}^0-\epsilon_i{}^0}\right)(\psi_\lambda | M^{-1/2}M_0{}^{1/2}f^{ui})\mathfrak{M}_{ig}{}^0\,.$$

Here, $\mathfrak{M}_{ug}{}^0, \mathfrak{M}_{ig}{}^0$ are the matrix elements of the dipole moment with respect to rigid-lattice wave functions $|\phi_u\rangle$, $|\phi_g\rangle$, $|\phi_i\rangle$; and $(\epsilon_u{}^0-\epsilon_i{}^0)$ is the difference in energy between the rigid-lattice electronic levels u and i.

When Eqs. (56) are inserted in the general expression for the characteristic function $I(t)$ of the absorption band,[2] after some trivial manipulations, one obtains

$$I(t) = \exp[-S(T) - i\Omega_{ug}t + \varphi(T;t)]\{|\mathfrak{M}_0|^2 + \textstyle\sum_\lambda (\mathfrak{M}_0\mathfrak{M}_\lambda\Delta_\lambda{}^* + \text{c.c.}) + \sum_\lambda |\mathfrak{M}_\lambda|^2[(n_T(\omega_\lambda)+1)e^{-i\omega_\lambda t} + n_T(\omega_\lambda)e^{i\omega_\lambda t}] + \sum_\lambda (\mathfrak{M}_0\mathfrak{M}_\lambda{}^*\Delta_\lambda + \text{c.c.})[n_T(\omega_\lambda)e^{i\omega_\lambda t} - (n_T(\omega_\lambda)+1)e^{-i\omega_\lambda t}] + \sum_{\lambda\lambda'} \mathfrak{M}_\lambda\Delta_\lambda{}^*\mathfrak{M}_{\lambda'}\Delta_{\lambda'}{}^*[1-(n_T(\omega_\lambda)+1)e^{-i\omega_\lambda t} + n_T(\omega_\lambda)e^{i\omega_\lambda t}][1-(n_T(\omega_{\lambda'})+1)e^{-i\omega_{\lambda'}t} + n_T(\omega_{\lambda'})e^{i\omega_{\lambda'}t}]\}\,. \tag{57}$$

Notice that, while $\mathfrak{M}_\lambda$ involves the nondiagonal field of force Eq. (5), Δ_λ, $S(T)$ and $\varphi(T;t)$ are again related to the diagonal part of the electron-phonon interaction.

Let be $\mathfrak{M}_{ug}{}^0 = 0$. The structure of the electric-dipole forced-absorption (emission) band depends, in a direct way, on the symmetry of the defect. A particularly simple situation occurs when the defect possesses cubic symmetry. Because the normal modes have different parity in Δ_λ and $\mathfrak{M}_\lambda$, respectively, all the terms that involve mixed products $\Delta_\lambda\mathfrak{M}_\lambda{}^*$ or $\Delta_\lambda{}^*\mathfrak{M}_\lambda$ drop out in expression (57). When the force-field Eq. (5) is analyzed according to the symmetry vectors $(lk|\alpha j)$, we are left with the simple form

$$I(t) = \exp[-S(T) - i\Omega_{ug}t + \varphi(T;t)]\textstyle\sum_{i\neq u}|\mathfrak{M}_{ig}{}^0|^2 \times\left(\dfrac{\hbar}{\epsilon_u{}^0-\epsilon_i{}^0}\right)^2 (1/\hbar)\sum_\alpha\sum_{jj'} f_{\alpha j}{}^{ui} f_{\alpha j'}{}^{iu}\int_0^\infty d\omega \times[(n_T(\omega)+1)e^{-i\omega t} + n_T(\omega)e^{i\omega t}]\rho_{\alpha jj'}(\omega^2)\,. \tag{58}$$

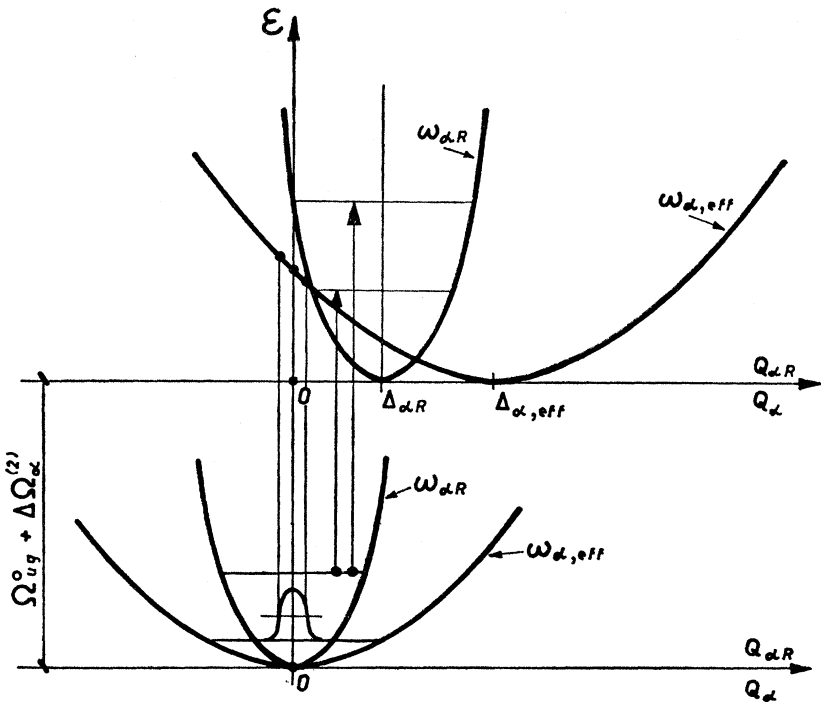

FIG. 5. Configurational diagram in the presence of both continuum and local modes. Notice that if $\int_0^\infty 2\omega\rho_\alpha{}^R(\omega^2)d\omega=1$ the continuum-modes parabola disappears.

As in Sec. II, the $f_{\alpha j}{}^{ui}$ in Eq. (58) denotes the mass-normalized force. We must, of course, project $|f^{ui})$ onto $|\mathrm{I};\alpha j)$ or on both $|\mathrm{I};\alpha j)$ and $|\mathrm{II};\alpha j)$, according to the range of the field of force. It turns out that the distribution function $I(\Omega)$ of the absorption band is the convolution of a many-phonon process with a one-phonon process; the many-phonon process is generated by the diagonal part of the electron-phonon interaction, while the one-phonon process is generated by the nondiagonal part. The most important feature is that no zero-phonon line results, and the lowest process is a one-phonon term.

The oscillator strength is found to be

$$f=\sum_{i\neq u}|\mathfrak{M}_{ig}{}^0|^2\left(\frac{\hbar}{\epsilon_u{}^0-\epsilon_i{}^0}\right)^2\left(\frac{1}{\hbar}\right)\sum_\alpha\sum_{jj'}f_{\alpha j}{}^{ui}f_{\alpha j'}{}^{iu}\times\int_0^\infty d\omega\,\rho_{\alpha jj'}(\omega^2)\coth(\hbar\omega/2k_BT). \quad (59)$$

Note that it depends explicitly on temperature. At $T\sim 0°\mathrm{K}$, the oscillator strength associated with the one-phonon term is easily seen to be equal to $\exp[-S(0)]$ multiplied by the oscillator strength of the whole phonon-forced band.

For low-symmetry centers, the above statements cannot be applied, and the expression in curly brackets on the right-hand side of Eq. (57) may also contain time-independent terms. This fact is reflected on the absorption (emission) band by a possible persistence of the zero-phonon line. Also multiple-phonon lines may, in principle, occur; it depends on the symmetry properties of the electron wavefunctions involved in the mixing of the upper state.

In dealing with the phonon-forced transitions, a particular role may be played by the polarization of light. The electric-dipole moment transforms, for centers of symmetry lower than the cubic, according to more than a single irr. rep. Therefore, some transitions which are dipole-allowed for unpolarized light may become dipole-forbidden for suitable polarization of light. In such a case, the transition can be electric-dipole forced by the phonons, and the above statements apply straightforwardly.

V. COMPARISON WITH EXPERIMENTAL DATA

A. Tightly Bound Electrons

As an example of tightly bound electrons, we consider the rare-earth (R.E.) ions in alkali halides. We choose Sm^{2+}. This ion gives rise to several absorption-emission bands, two of which show a peculiar structure.[6] The former band is detected in emission, and corresponds to the intraconfigurational transition ${}^5D_0(A_1)\rightarrow{}^7F_0(A_1)$ of the ion. The latter is usually detected in absorption, and corresponds instead to the intraconfigurational transition $(4f)^6\rightarrow(4f)^5 5d$. Their Huang-Rhys parameters, as experimentally observed for Sm^{2+} in KCl at $T\simeq 10°\mathrm{K}$, are about $S=1$ and $S=5$, respectively.[25] As a positive-ion vacancy associates with the R.E. ion at low temperature, both the intraconfigurational and the interconfigurational transitions become dipole-allowed

[25] G. Baldini and M. Guzzi (private communication).

TABLE II. Pseudolocal-mode frequencies, $\omega_{R,1}$ and $\omega_{R,2}$, for Sm^{2+} in NaCl, KBr, and RbCl at 5°K.

	$(\omega_{R,1})_{exp}$ (10^{13} sec^{-1})	$(\omega_{R,2})_{exp}$ (10^{13} sec^{-1})	$(\omega_{R,1})_{th}$ (10^{13} sec^{-1})	λ[a]
NaCl	0.97[b]	4.1[b]	0.95	1.5
KBr	0.74[b]	2.85[b]	0.7	1.3
RbCl	0.73[b]	3.63[b]	0.7	1.1

[a] In units of perfect lattice force constant. See G. Benedek and G. F. Nardelli, Phys. Rev. 155, 1004 (1967).
[b] From Ref. 7.

because of the low-symmetry crystal field. The vibrational structures of these bands were recently considered by Bron and Wagner.[6] However, these authors did not present, in our opinion, a satisfactory explanation of the marked difference between the structure observed in the interconfigurational and the intraconfigurational transitions.

The lattice dynamics of the R.E. ion-vacancy system in alkali halides has been considered by the above authors, therefore we do not report any details of it. We simply remark that to neglect the off-diagonal matrix elements of the unperturbed phonon propagator is a crude approximation, for these elements are responsible for the effects that the positive ion vacancy induces in the system, in the low-frequency region. We have considered these effects by using the usual device[26]: adding a fictitious particle to the lattice and evaluating the spectral density with this particle included. This particle is then decoupled from the lattice by letting its mass go to infinity. In such a way, the three additional degrees of freedom that we have added to our system are reflected on the frequency spectrum by a threefold degenerate resonant mode at zero frequency, and can be divided out. The possible pseudolocal or local modes involved in the transition display A_1 symmetry; this fact corresponds to considering the augmented perturbation

$$\bar{\Lambda}_{A_1}(\omega^2)\equiv\begin{vmatrix}(\lambda/M_+)+\epsilon\omega^2 & -\lambda/(M_+M_-)^{1/2} & \sim 0\\ -\lambda/(M_+M_-)^{1/2} & \lambda/M_- & \sim 0\\ \sim 0 & \sim 0 & \epsilon'\omega^2\end{vmatrix} \quad (60)$$

in the defect model adopted by Bron and Wagner. $\epsilon=-(M_{++}-M_+)/M_+$ is the fractional change of mass due to the (R.E.) ion, and λ the change of force constant. $\epsilon'\omega^2$ accounts for the effects of the positive-ion vacancy in the limit $\epsilon'\to-\infty$. The perturbed projected density of states $\bar{\rho}_{A_1}(\omega^2)$ splits as

$$\bar{\rho}_{A_1}(\omega^2)=\rho_{A_1}(\omega^2)+\rho_{A_1}{}^{(\epsilon')}(\omega^2), \quad (61)$$

where $\rho_{A_1}(\omega^2)$ is a 2×2 matrix in the space of the first two symmetry coordinates, and $\rho_{A_1}{}^{(\epsilon')}(\omega^2)=(1/|\epsilon'|)\delta(\omega^2)$ is a 1×1 matrix in the space of the last symmetry coordinate. The factor $(1/|\epsilon'|)$ comes from the normalization property of the projected densities. For Sm^{2+}, $\rho_{A_1}(\omega^2)$ turns out to have an area of the order of $M_+/M_{Sm^{2+}}$, coming from the normalization conditions (A17), and furthermore its resonant part was found to be a considerable fraction of this same area.

[26] G. F. Nardelli and N. Tettamanzi, Phys. Rev. 126, 1283 (1962).

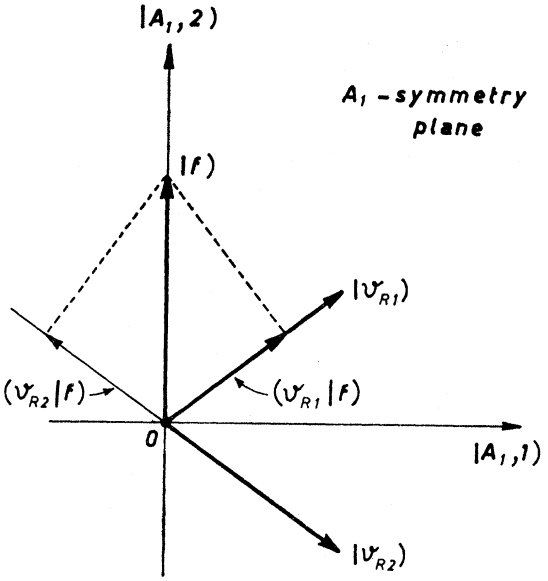

FIG. 6. Relative position of the low- and high-frequency resonant modes with respect to the A_1-symmetry component of the force.

The eigenvector equation of the resonant modes of A_1 symmetry is considered in the above 2×2 subspace. The result is shown in Fig. 6: $|A_1,1)$ and $|A_1,2)$ are the involved symmetry vectors (see Appendix); $|v_{R1})$ and $|v_{R2})$ are the low-frequency and high-frequency resonant vectors, respectively. In qualitative accordance with Wagner's prediction, we find that, having once taken the limit $\epsilon'\to-\infty$, at least two resonances occur for fairly large and positive λ. The low-frequency resonance is, however, considerably lowered by the positive-ion vacancy. The comparison between experimental and theoretical frequencies is shown in Table II. After some calculations, we further obtain

$$\frac{(1,A_1|v_R)}{(2,A_1|v_R)}=\begin{cases}(M_+/M_-)^{1/2} & \text{low-freq. mode}\\ \sim-(M_+/M_-)^{1/2}, & \text{high-freq. mode,}\end{cases} \quad (62)$$

where $(j,A_1|v_R)$, $j=1,2$, are the components of the resonant vector in the 2×2 subspace (see Appendix). The situation is shown in Fig. 6.

As regards the field of force, it is known[6] that the $^5D_0(A_1)\to{}^7F_0(A_1)$ intraconfigurational transition gives rise essentially to a dipole field, say $\mathbf{E}^{(d)}$, while on the other hand the $(4f)^6\to(4f)^5 5d$ interconfigurational transition gives rise to both dipole and quadrupole fields of force, i.e., $\mathbf{E}^{(d)}+\mathbf{E}^{(Q)}$, the former being in the region spanned by $\bar{\Lambda}(\omega^2)$, two orders of magnitude smaller than the latter. In this region, these fields display A_1 symmetry; furthermore, both $\mathbf{E}^{(d)}$ and $\mathbf{E}^{(Q)}$ lie in the $(A_1,2)$ direction, which is quite different from

those of both the low-frequency and the high-frequency resonant eigenvectors [$|v_{R,1}\rangle$ and $|v_{R,2}\rangle$, respectively] in those crystals for which $M_+ \gg M_-$ (see Fig. 6). Then, only the interconfigurational transition is able to activate, through the quadrupole field $\mathbf{E}^{(Q)}$, the two localized modes in region (I).

A particular situation occurs for the ${}^5D_0(A_1) \rightarrow {}^7F_0(A_1)$ transition. The off-direction situation at short range, together with the peculiar behavior of the dipole field considered far from the defect, make the unperturbed phonons enter mainly the expression for $\varphi(T;t)$. This explains the main difference between the ${}^5D_0(A_1) \rightarrow {}^7F_0(A_1)$ and the $(4f)^6 \rightarrow (4f)^5 5d$ transitions. Far from the defect, the dipole field vanishes when averaged over spherical shells, so we can write

$$\lim_{\epsilon' \rightarrow -\infty} (f|\delta(\omega^2 - L_0 - \bar{\Lambda}(\omega^2))|f) \approx (f_{\mathrm{I}}|\rho_{A_1}(\omega^2)|f_{\mathrm{I}}) + (f_{\mathrm{II}}|\rho^0(\omega^2)|f_{\mathrm{II}}). \quad (63)$$

Furthermore, $\rho_{A_1}(\omega^2)$ splits according to Eq. (A13). For both low- and high-frequency resonances, $|f_{A_1})$ falls noticeably in off-direction; the short-range part of the dipole field is therefore unable to activate the resonant modes. This permits us to consider the continuum-phonon part only, $\rho_{A_1}{}^c(\omega^2)$, in the first term on the right-hand side of Eq. (63). Without error, we can further replace $\rho_{A_1}{}^c(\omega^2)$ by $\rho_I{}^0(\omega^2)$ and write

$$\lim_{\epsilon' \rightarrow -\infty} (f|\delta(\omega^2 - L_0 - \bar{\Lambda}(\omega^2))|f) \approx (f|\delta(\omega^2 - L_0)|f)$$
$$= M_+ \sum_{\kappa\kappa'} \sum_{\mathbf{q}} \mathbf{d} \cdot \mathbf{L}_0{}^C(\mathbf{q};+,\kappa) \times \delta(\omega^2 - \mathbf{L}_0(\mathbf{q};\kappa\kappa'))\mathbf{L}_0{}^C(\mathbf{q};\kappa',+) \cdot \mathbf{d}$$
$$= \sum_s \langle |f_{s\mathbf{q}}|^2 \rangle_{\omega^2}{}^{(s)} \rho_s{}^0(\omega^2). \quad (64)$$

We have made use of Eqs. (7) and (8), and we have put

$$f_{s\mathbf{q}} \equiv (s,\mathbf{q}|f) = (\boldsymbol{\varepsilon}_{s\mathbf{q}}|L_0{}^C(\mathbf{q})|\mathbf{d})M_+{}^{1/2}. \quad (65)$$

For the other symbols see the Appendix. The one-phonon component of $I(\Omega)$ is then expected to display vibrational structures closely related to the spectral density of the unperturbed host lattice. At low frequency (i.e., near the zero-phonon line), only the acoustic branches (i.e., $s=A$) contribute to Eq. (64), so that

$$\langle |f_{s\mathbf{q}}|^2 \rangle_{\omega^2 \rightarrow 0}{}^{(A)} \sim (\omega_A{}^C)^2 \sim (0^+)^4, \quad (66)$$

where $\omega_A{}^C$ is the acoustic frequency as given by the pure Coulomb interaction in the host lattice. Equation (66) explains the low-frequency discrepancy observed between the spectral density of the unperturbed lattice and the one-phonon side band of the ${}^5D_0(A_1) \rightarrow {}^7F_0(A_1)$ transition.

Finally, we add some remarks on the electric dipole forced transitions of Sm^{2+} in CaF_2 [27] and $SrCl_2$.[28] In these crystals, Sm^{2+} does not affect the host-crystal O_h point symmetry. No zero-phonon lines are then expected in such transitions, since the mixed terms $\mathfrak{M}_\lambda \Delta_\lambda$ in Eq. (57) vanish for symmetry reasons. In the particular case of transition ${}^5D_0(A_{1g}) \rightarrow {}^7F_0(A_{1g})$, only the exchange interaction, which is indeed very weak, can contribute to the "diagonal" part of the electron-phonon interaction; therefore, $\exp[-S+\varphi(t)] \sim 1$ and no many-phonon process occurs. Furthermore, the field of force entering the "nondiagonal" part of the electron-phonon interaction is essentially of dipole type. By analogy with the ${}^5D_0(A_1) \rightarrow {}^7F_0(A_1)$ transition in the alkali halides, we can then conclude that the phonon forced transition ${}^5D_0(A_{1g}) \rightarrow {}^7F_0(A_{1g})$ in both CaF_2 and $SrCl_2$ essentially display the vibrational structures of the unperturbed spectral density of the host lattice.

A different situation is expected for the ${}^5D_0 \rightarrow {}^7F_2$ electric dipole forced transitions of Sm^{2+} in ZnS crystals. As the point group of this crystal (O cubic group) does not include the inversion symmetry, ${}^5D_0$ transforms according to the A_1 irr. rep. while ${}^7F_2$ splits into ${}^7F_2(E)$ and ${}^7F_2(T_2)$. The "nondiagonal" part of the electron-phonon interaction mixes ${}^7F_1(T_1)$ with either ${}^7F_2(E)$ or ${}^7F_2(T_2)$. This allows the transition from ${}^5D_0(A_1)$. For transition ${}^5D_0(A_1) \rightarrow {}^7F_2(E)$, again the zero-phonon line does not occur, because Δ_λ and $\mathfrak{M}_\lambda$ in Eq. (57) involve phonons of symmetry A_1, A_2, E, and T_1, T_2, respectively. However, for the transition ${}^5D_0(A_1) \rightarrow {}^7F_2(T_2)$, phonons of symmetry E, T_1 and T_2 occur in both Δ_λ and $\mathfrak{M}_\lambda$ so that the zero-phonon line is expected there. A similar situation should appear in crystals displaying T_d point symmetry.

B. *F*-Center

We recall $S(T) \equiv \varphi(T;t=0)$. From (17), one obtains

$$S(T) = \frac{1}{\hbar} \sum_\alpha{}^{(+)} \sum_{jj'} f_{\alpha j} f_{\alpha j'} \int_0^\infty d\omega \times \omega^{-2} \rho_{\alpha jj'}(\omega^2) \coth \frac{\hbar\omega}{2K_B T}, \quad (67)$$

while in Gaussian approximation, the peak position $\bar{\Omega}(T)$ and halfwidth $H(T)$ of the absorption band turn out to be, up to a quadratic coupling approximation,

$$\bar{\Omega}(T) = \Omega_{u_g}{}^0 + \Delta\Omega^{(1)} + \Delta\Omega^{(2)}, \quad (68)$$

$$\Delta\Omega^{(1)} \simeq \frac{1}{\hbar} \sum_\alpha{}^{(+)} \sum_{jj'} f_{\alpha j} f_{\alpha j'} \int_0^\infty d\omega\, \omega^{-1} \rho_{\alpha jj'}(\omega^2), \quad (69)$$

where $\Delta\Omega^{(2)}$ is given in (20), and

$$H^2(T) = [H^{(1)}(T)]^2 + [H^{(2)}(T)]^2, \quad (70)$$

$$[H^{(1)}(T)]^2 = (8 \ln 2) \frac{1}{\hbar} \sum_\alpha{}^{(+)} \sum_{jj'} f_{\alpha j} f_{\alpha j'} \int_0^\infty d\omega \times \rho_{\alpha jj'}(\omega^2) \coth \frac{\hbar\omega}{2K_B T}, \quad (71)$$

[27] J. D. Axe and P. P. Sorokin, Phys. Rev. **130**, 945 (1963).
[28] D. L. Wood and W. Kaiser, Phys. Rev. **126**, 2079 (1962).

TABLE III. Theoretical values of $\Delta\Omega^{(1)}$ and $\Delta\Omega^{(2)}$ for F center absorption band at $T=5°K$. $\hbar\Omega_{ug}{}^0$ is the energy of the pure electronic transition as deduced by subtracting $\Delta\Omega^{(1)}$ and $\Delta\Omega^{(2)}$ at $T=5°K$ from Ω_{exp}.

	$\hbar\Delta\Omega^{(1)}{}_{th}$ (eV)	$\hbar\Delta\Omega^{(2)}{}_{th}$ (eV)	$\hbar\Omega_{exp}$ (eV)	$\hbar\Omega_{ug}{}^0=\hbar\Omega_{exp}-\hbar(\Delta\Omega^{(1)}+\Delta\Omega^{(2)})$ (eV)
NaCl	0.6[a]	−0.05[b]	2.77[c]	2.22
KCl	0.3[a]	−0.02[b]	2.31[c]	2.03

[a] From Eq. (69) in the text.
[b] From Eq. (20) in the text.
[c] J. J. Markham and J. D. Konitzer, J. Chem. Phys. 32, 843 (1960); 34, 1936 (1961).

$$[H^{(2)}(T)]^2=(\tfrac{1}{2}\ln 2)\int_{-\infty}^{\infty}d\omega\int_{0}^{\infty}d\omega'\times\left\{\mathrm{Tr}\{\Lambda^{(2)}\rho(\omega'^2)\Lambda^{(2)}\rho((\omega-\omega')^2)\}\theta(\omega-\omega')\times\left[1+\coth\left(\frac{\hbar(\omega-\omega')}{2K_BT}\right)\coth\left(\frac{\hbar\omega'}{2K_BT}\right)\right]+\mathrm{Tr}\{\Lambda^{(2)}\rho((\omega+\omega')^2)\Lambda^{2}\rho(\omega'^2)\}\theta(\omega+\omega')\times\left[\coth\left(\frac{\hbar(\omega+\omega')}{2K_BT}\right)\coth\left(\frac{\hbar\omega'}{2K_BT}\right)-1\right]\right\}. \tag{72}$$

The superscript (+) on the summation in the right-hand side of Eqs. (67), (69), and (71) means summation over the even irr. reps. of the defect point group.

We do not go into details of the calculations of the above quantities as they are reported elsewhere in connection with infrared absorption and Raman scattering,[29] with a detailed analysis of the ground-state vibrational properties of the F center. We simply remark that the forces $f_{\alpha j}$ can be deduced from the hydrostatic, trigonal, and tetragonal stress coefficients $\mathcal{A}$, $\mathfrak{B}$, and $\mathfrak{C}$ of the absorption band.[11,12] Insofar as quadratic and higher-order terms of the electron-phonon interaction can be disregarded, the frequency shift of the band peak, under the action of an external stress, just corresponds to the energy shift of the zero-phonon line. It turns out that the stress coefficients, as usually measured, represent the derivative of the hole-electron pair energy with respect to the applied strain or, apart from some numerical factor, exactly the forces in Eq. (3) for the symmetries involved. We have simply

$$f_{A_{1g}}=\frac{\mathcal{A}}{\tilde{r}_0M_+^{1/2}}(\tilde{c}_{11}+2c_{12}),\quad f_{E_g,t}=\frac{\mathfrak{B}}{\tilde{r}_0M_+^{1/2}}(\tilde{c}_{11}-c_{12}),$$
$$f_{T_{2g}}=\frac{\mathfrak{C}}{\tilde{r}_0M_+^{1/2}}(\tilde{c}_{44}),\qquad f_{E_g,r}=\frac{3\mathfrak{B}}{\tilde{r}_0M_+^{1/2}}(\tilde{c}_{11}-c_{12}). \tag{73}$$

[29] G. Benedek and E. Mulazzi (to be published). See also E. Mulazzi and N. Terzi, J. Phys. Radium 28, C4-49 (1967).

The labels t or r on E_g mean tetragonal or rhombic, respectively. $\tilde{c}_{ij}$ and c_{ij} denote local and bulk elastic constants, respectively.[30] $\tilde{r}_0$ is the equilibrium distance between the F-center lattice site and its nearest neighbors (n.n.) in the ground-state relaxed configuration. $\mathcal{A}$, $\mathfrak{B}$, and $\mathfrak{C}$ are related by

$$\mathcal{A}=\tfrac{1}{3}\mathfrak{A}_1,\quad \mathfrak{B}=\tfrac{1}{6}\mathfrak{A}_{3a},\quad \text{and}\quad \mathfrak{C}=\mathfrak{A}_{5a}$$

to the Schnatterly stress coefficients $\mathfrak{A}_1$, $\mathfrak{A}_{3a}$, and $\mathfrak{A}_{5a}$.[11] The evaluated halfwidth and Huang-Rhys parameter[29] are found to be in good agreement with the experimental data. We report here only the results on the phonon contribution to the peak energy in NaCl and KCl crystals (see Tables III and IV). The $\Delta\Omega^{(2)}$ has been evaluated with the help of Eqs. (10) and (20), assuming the values reported in Ref. 31 for the electron charge redistribution during the $s\rightarrow p$ transition. We assumed that $\Delta\Omega^{(1)}$ in Eq. (69) depends on temperature essentially through $f_{\alpha j}$, while the main temperature variation of $\Delta\Omega^{(2)}$ comes from $\coth(\hbar\omega_{\mathrm{eff}}/2K_BT)$. From Table III, it appears that $\Delta\Omega^{(2)}$ is a small fraction of $\Delta\Omega^{(1)}$ at $T=5°K$; however, it depends on T more than $\Delta\Omega^{(1)}$ (Table IV). We find that both $\Delta\Omega^{(1)}$ and $\Delta\Omega^{(2)}$ give a contribution to the temperature shift of the peak position which is of the same order of magnitude. They account for the temperature shift as actually observed. This fact suggests that $\Omega_{ug}{}^0$ in Eq. (68) does not depend appreciably on temperature. It is worth noticing that $\hbar\Omega_{ug}{}^0$ represents the difference of energy between the minimum of the electronic upper state in the "displaced" configuration [i.e., $\epsilon_u{}^0(\Delta_\lambda)+\hbar\Delta\Omega^{(2)}$] and the minimum of the ground state in the relaxed (equilibrium) configuration [i.e., $\epsilon_g{}^0(0)$] (see, however, Sec. VI).

A peculiar behavior is expected for the temperature shift when the temperature variations of $\Delta\Omega^{(1)}$ and $\Delta\Omega^{(2)}$ differ in sign. This could explain the anomalies that the temperature shift displays in some centers, such as certain aggregates of F centers.[32]

VI. CONCLUSIONS AND FINAL REMARKS

In the present analysis, we have chosen as coupling constants of the electron-phonon interaction the set of mass-normalized forces $f_{\alpha j}$ which the "hole-electron pair" exerts on the surrounding crystal lattice. We can then foresee the most important features of the absorption (emission) band, without performing any explicit calculations. For instance, it is possible to foresee well-marked vibrational structures for all the optic transitions that occur between tight-bound or atomic-like wave functions, as is the case of rare-earth ions, molecular centers, and transition metals in alkali and alkaline-earth halides; it is further possible to explain

[30] G. Benedek and G. F. Nardelli, Phys. Rev. 167, 837 (1968).
[31] G. Iadonisi and B. Preziosi, Nuovo Cimento 48, 92 (1967).
[32] Y. Farge, G. Toulouse, and M. Lambert, J. Phys. Radium 28, C4-66 (1967).

TABLE IV. Vibrational contributions, $\Delta\Omega^{(1)}(T)$ and $\Delta\Omega^{(2)}(T)$, to the peak position of the F-center absorption band at different temperatures.

		$\hbar[\Delta\Omega^{(1)}(T)-\Delta\Omega^{(1)}(5°K)]_{th}$ (eV)	$\hbar[\Delta\Omega^{(2)}(T)-\Delta\Omega^{(2)}(5°K)]_{th}$ (eV)	$\hbar[\Delta\Omega(T)-\Delta\Omega(5°K)]_{th}$ (eV)	$\hbar[(T)\bar{\Omega}-\bar{\Omega}(5°K)]_{exp}$ (eV)
NaCl	$T=180°K$	-2.5×10^{-2}	-1.5×10^{-2}	-4×10^{-2}	-4.5×10^{-2} [a]
	$T=300°K$	-5×10^{-2}	-4×10^{-2}	-9×10^{-2}	-9.9×10^{-2} [a]
KCl	$T=200°K$	-3×10^{-2}	-2×10^{-2}	-5×10^{-2}	-5.2×10^{-2} [a]
	$T=300°K$	-4.8×10^{-2}	-3.2×10^{-2}	-8×10^{-2}	-8.7×10^{-2} [a]

[a] J. J. Markham and J. K. Konitzer, J. Chem. Phys. 32, 843 (1960); 34, 1936 (1961).

why aggregate of defects, such R,N,M centers in alkali halides, and, perhaps, some trapped excitons may fall into an intermediate case.

It may be interesting to note that most of the considerations we have given the absorption (emission) transition can be easily applied to the Raman activity of the imperfect, or perfect, crystals. Essentially, we must replace the forces by the electronic polarizability tensors $P_{\alpha\beta}(l,\kappa)$ in the definition of the phonon-structure function Eq. (16),[12] and keep in mind that, as the Raman scattering involves only virtual electronic transitions, the phonon-structure function does not appear through an exponential factor.

In our description, zero- and multiple-phonon lines are formally treated as δ functions. Actually, the zero-phonon line behaves essentially as a Lorentzian whose halfwidth, as limited by the quadratic electron-phonon interaction, is

$$\Gamma=(\tfrac{1}{16}\pi)\int_0^\infty d\omega \times\mathrm{Tr}\{\Lambda^{(2)}\rho(\omega^2)\Lambda^{(2)}\rho(\omega^2)\}\left[\coth^2\left(\frac{\hbar\omega}{2K_BT}\right)-1\right].$$

Of course, we should include also the contributions from the lifetime of the electronic excited state and from anharmonicity. Since every multiple-phonon line is generated by the zero-phonon line of the continuum-phonon process [see Eqs. (28) and (29)], every line is expected to display Lorentzian shape, with practically the same halfwidth. The central question is that of the reliability of treating the possible pseudolocal-mode by δ functions. While this is quite valid for local modes as well as for exceptionally sharp resonances (mainly in the low-acoustic region), it seems to us that ill-defined resonances are more suitably treated as defect-induced structures in the continuum part [see $\rho_\alpha{}^c(\omega^2)$ in the text] of the projected density of states. In such a case they should appear as less sharp vibrational structure of the continuum-phonon distribution function $I_c(\Omega)$, and, in general, they then do not display Lorentzian shape. Furthermore, they should not display an accentuated multiple-phonon character.

As to the effects of temperature, a finite temperature is not solely responsible for the broadening of the vibrational structures (if any). Indeed, when the temperature is not extremely low, Stokes as well as anti-Stokes lines should be expected in the absorption band. Recent observations seem to account for such lines.[25]

With regard to the configuration diagram, we have shown that this description does not allow for any detailed interpretation of the many-phonon process beyond the first and second moments of the distribution function $I(\Omega)$ of the absorption (emission) band. In order to account, at least qualitatively, for both the asymmetry and the exponential tail of the band, we must consider the short-time expansion of $\varphi(T;t)$ up to the third order. In this way, the exponential tail arises as result of a crystal-field effect on the electron wave function in the "displaced" (not "relaxed") configuration.

In the use of the configuration diagram, a limitation exists when a local (pseudolocal) mode of allowed symmetry exists. For this mode, the projected normal coordinate $Q_{\alpha R}$ is essentially the exact normal coordinate Q_α, if the perturbed projected density of states is very small in practically the whole frequency range with the exception of a narrow interval around the resonance frequency ω_R. The diagram of Fig. 5 would lead to a deceiving description of the many-phonon process, even if $S(0)\gg1$. Indeed, Eq. (28) implies that, at low temperature, the local mode may induce sharp and well resolved multiple-phonon lines.

We add some remarks on the Stokes shift between absorption and emission bands of the F center. On the plot of Fig. 4 we have reported the usual adiabatic energy functions $\epsilon_u{}^0(Q_\alpha)$ and $\epsilon_g{}^0(Q_\alpha)$, as well as a hypothetic energy function $\tilde{\epsilon}_g(Q_\alpha)$. The distinction between $\tilde{\epsilon}_g{}^0(Q_\alpha)$ and $\epsilon_g{}^0(Q_\alpha)$ concerns the polarization field of the crystal lattice.[33]

The polarization splits as

$$\mathbf{P}_{tot}=\mathbf{P}_{el}+\mathbf{P},$$

[33] Of course, we should consider the Jahn-Teller effect (i.e., the effects due to the "nondiagonal" part of the dectron-phonon interaction) if the electronic quantum state is degenerate. This later effect has been extensively considered in Refs. 22 and 23.

where $\mathbf{P}$ is the infrared component of the polarization field. Both $\mathbf{P}_{el}$ and $\mathbf{P}$ enter the definition of the electronic excitation[34]; however, the time scale on which they interact with the electron are quite different, the electronic component $\mathbf{P}_{el}$ operating on the time scale of the fast electrons. $\mathbf{P}_{el}$ enters straightforwardly into the definition of the adiabatic energy function of the electronic upper state (the so-called "electronic polaron")[35]; $\mathbf{P}_{el}$ should instead be excluded from the definition of the ground state, as there the electron behaves as a fairly fast electron. $\mathbf{P}_{el}$ must be determined self-consistently with respect to the quantum state of the electron. Then, it may happen that a modified ground level, with a corresponding adiabatic energy function $\tilde{\epsilon}_g(Q_\alpha)$, exists in the electronically polarized lattice. It turns out that the Stokes shift, usually measured as the energy difference between peak positions of absorption and emission bands, splits into two terms: a purely Stokes term and a stored-energy term. The former corresponds to the energy dissipated by Stokes phonons and amounts to

$$\hbar[\Delta\Omega_{em}{}^{(1)}+\Delta\Omega_{em}{}^{(2)}]+\hbar[\Delta\Omega_{ab}{}^{(1)}+\Delta\Omega_{ab}{}^{(2)}]$$

[see Eqs. (20) and (69)]. The latter represents the amount of energy involved in the electronic polarization of the host lattice (see also Ref. 36). This stored energy should be given by $\hbar[(\Omega_{ug}{}^0)_{ab}-(\Omega_{gu}{}^0)_{em}]$, i.e., by the difference in energy between the pure electronic transitions (essentially the zero-phonon lines, when resolved) for absorption and emission. It seems to us that this term, i.e., the Stokes shift as corrected by removal of the purely Stokes term, contains the most relevant information on the lattice polarizability. When we subtract (add) the quantity $\Delta\Omega_{ab}{}^{(1)}+\Delta\Omega_{ab}{}^{(2)}$ ($\Delta\Omega_{em}{}^{(1)}+\Delta\Omega_{em}{}^{(2)}$) from (to) the peak frequency $\bar{\Omega}$ of the absorption (emission), we find that $(\Omega_{ug}{}^0)_{ab}$ is, in fact, not equal to $(\Omega_{gu}{}^0)_{em}$. Furthermore, when $\hbar[(\Omega_{ug}{}^0)_{ab}-(\Omega_{gu}{}^0)_{em}]$, thus deduced, is plotted against $1/\epsilon=1/\epsilon_\infty-1/\epsilon_0$, a fairly good linear relationship is achieved (see Fig. 7). In Fig. 7 we have considered only the alkali halides for which the F center absorption (emission) band[37] displays a fairly good Gaussian shape, and for which the Jahn-Teller effect is probably negligible.[38] In the evaluation of $\Delta\Omega^{(1)}$, the essential point is to use the relationship that we found between the coupling constants $f_{\alpha j}$ and hydrostatic, trigonal, and tetragonal stress coefficients $\mathcal{A}$, $\mathfrak{B}$, and $\mathfrak{C}$ of the absorption band.

With regard to electronic transitions in crystals other than the transitions of a trapped electron, the results of the present paper apply straightforwardly.

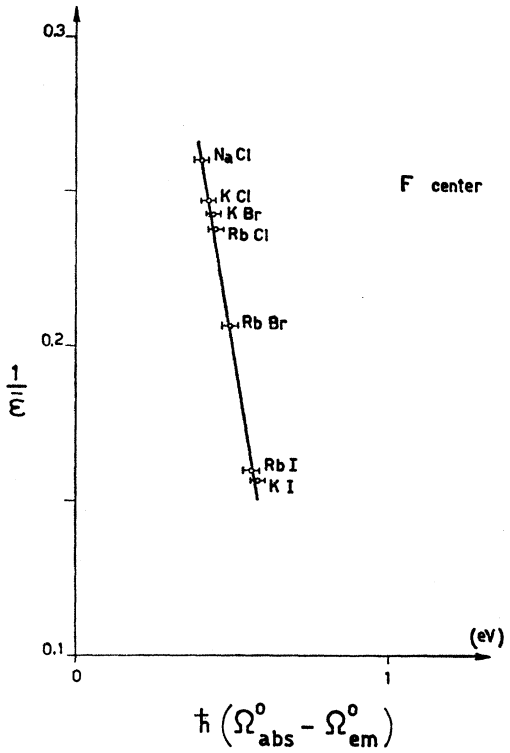

FIG. 7. Self-energy term of the F-band Stokes shift versus $1/\epsilon=1/\epsilon_\infty-1/\epsilon_0$.

The exciton absorption is one such example, as the exciton Hamiltonian in the center-of-mass system reads quite similarly to the Hamiltonian for the phonon-interacting hole-electron pair, which we considered in dealing with trapped electrons.[39–41] In this case, we must, however, project the unperturbed density of states onto the region of the crystal lattice on which the exciton applies non-negligible forces. In order to account for the exciton translational degree of freedom we simply must consider a configuration diagram (see Fig. 8) with one more axis, on which we plot the exciton wavevector $\mathbf{K}$. In this way, while the many-phonon process is represented on the (ϵ,Q_α) plane, the phonon assisted process,[41,42] i.e., the process that involves the center-of-mass coordinate (wavevector conservation $\mathbf{q}=\mathbf{K}$), is analyzed in the $(\epsilon,\mathbf{K})$ plane. The coupling constants for the latter process correspond to force field Eq. (5), where $|\phi_u\rangle$ represents now the center-of-zone exciton and $|\phi_i\rangle$ the exciton travelling with wavevector $\mathbf{K}$. For excitons in the alkali halides, the most relevant plane seems to be the plane involving the projected coordinate Q_α. Because of the large change that the orbit radius of the electron undergoes during the exciton

[34] As we are considering optic transitions that fall quite far from the infrared region, the optic electron is assumed to carry out the quantum transition in a time interval which is extremely short on the time scale of the lattice dynamics.

[35] Y. Toyozawa, Progr. Theoret. Phys. (Kyoto) **12**, 421 (1954); H. Haken and W. Schottky, Z. Physik. Chem. **16**, 218 (1958); M. Frolich, Advan. Phys. **3**, 325 (1954).

[36] W. B. Fowler, Phys. Rev. **135**, A1725 (1964).

[37] P. Podini and G. Spinolo (unpublished data).

[38] P. R. Moran, Phys. Rev. **137**, 1016 (1965).

[39] J. Hermanson and J. C. Phillips, Phys. Rev. **150**, 652 (1966).

[40] G. D. Mahan, Phys. Rev. **145**, 602 (1966).

[41] R. S. Knox, in *Solid State Physics*, edited by F. Seitz and D. Turnbull (Academic Press Inc., New York, 1963), Suppl. 5, p. 146.

[42] B. Segall, Phys. Rev. **150**, 734 (1966).

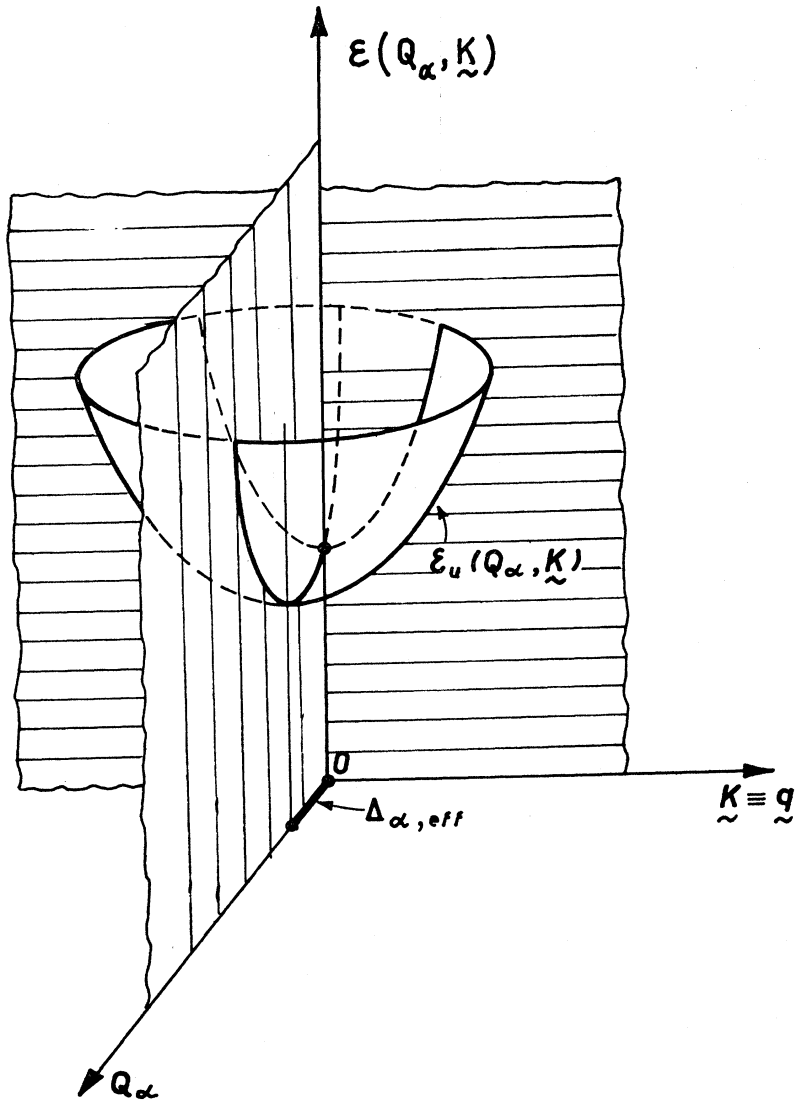

FIG. 8. Configurational diagram for the intrinsic exciton transition (absorption). The origin represents the vacuum state of the exciton.

transition, the first exciton peak is expected to behave quite similarly to the F band. Notice that the self-trapping of the hole resulting from the lattice relaxation would prevent the exciton from traveling through the lattice. In semiconductors the situation is reversed and the phonon assisted process [$(\epsilon,\mathbf{K})$ plane] should play the most relevant role. Generally the absorption band is a convolution of a many-phonon process with a phonon-assisted process.

An exciton trapped in a crystal imperfection probably behaves as a weakly bound electron. The peculiar properties of the imperfect lattice dynamics may then appear in the absorption band as resolved structures.

The last remark concerns the absorption edge in Perovskite-type crystals. In these crystals, the electronic excitations might induce a local instability of the crystal lattice. The dielectric constant is very large, and the orbit radius of the hole-electron pair is expected to be considerably large. The lattice relaxation around the electronic excitation might then lead to a sort of exciton-coupled local lattice transformation, with the net result of providing a well-oriented local electric field. Since part of this process may occur during the optic transition itself, a local electric field[43] could assist the transition, giving rise to a sort of intrinsic Franz-Keldish effect. This would then account straightforwardly for the marked exponential edge, which the absorption displays in these crystals.

ACKNOWLEDGMENTS

We are glad to acknowledge the interesting discussions on the F center with G. Spinolo, and to thank him and P. Podini for allowing us to use unpublished experimental data.

[43] D. Redfield, Phys. Rev. **130**, 916 (1963).

APPENDIX: LATTICE DYNAMICS

In this Appendix, we analyze in detail the imperfect lattice dynamics without any explicit reference to the electron-phonon interaction; labels (g) or (u) are therefore irrelevant.

With λ, we label the normal imperfect lattice modes including wavelike as well as local and pseudolocal modes. They obey the usual equation

$$(L-\omega_\lambda^2)\psi_\lambda=0, \tag{A1}$$

where ω_λ is the circular frequency and L the dynamical matrix. The matrix L is related by

$$\begin{aligned}L(l\kappa,l'\kappa')&=M_{l\kappa}^{-1/2}\Phi(l\kappa,l'\kappa')M_{l'\kappa'}^{-1/2}\\&=(\kappa l|M^{-1/2}\Phi M^{-1/2}|l'\kappa')\end{aligned} \tag{A2}$$

to the force-constant matrix Φ of the imperfect lattice.

$M_{l\kappa}$ is the ion mass at the $(l\kappa)$ lattice site of the imperfect crystal (M in matrix notation); l labels N primitive cells and κ the ions within the primitive cell. In writing the last equality in Eq. (A2), we introduced the linear-vector-space notation, and denoted by $|l\kappa,x)$ the basis vector, which corresponds one-to-one to the x Cartesian component of the lattice displacement from the $(l\kappa)$th lattice site (lattice displacement representation). In Eq. (A2), the Cartesian component x was understood. We require these unit vectors to be mutually orthogonal, so that we can represent the whole set of lattice displacements by a vector $|u)$ of this space through the relation

$$|u)=\sum_{l\kappa x}u_{l\kappa x}|l\kappa,x), \tag{A3}$$

where $u_{l\kappa x}$ is the xth Cartesian component of the $(l\kappa)$ ion displacement. The normal modes are assumed to satisfy the usual orthonormality and closure conditions

$$\begin{aligned}&\sum_{l\kappa}\psi_\lambda^*(l\kappa)\cdot\psi_{\lambda'}(l\kappa)\\&\quad=\sum_{l\kappa}(\psi_\lambda|l\kappa)\cdot(l\kappa|\psi_{\lambda'})=(\psi_\lambda|\psi_{\lambda'})=\delta_{\lambda,\lambda'},\end{aligned} \tag{A4a}$$

$$\begin{aligned}&\sum_\lambda\psi_\lambda^*(l\kappa)\psi_\lambda^*(l'\kappa')\\&\quad=\sum_\lambda(l\kappa|\psi_\lambda)(\psi_\lambda|l'\kappa')=(l\kappa|l'\kappa')=\delta_{l,l'}\delta_{\kappa,\kappa'}\mathbf{1},\end{aligned} \tag{A4b}$$

where we have put $\psi_\lambda(l\kappa)\equiv(l\kappa|\psi_\lambda)$, and we have denoted by means of $\mathbf{1}$ the unit dyadic.

From Eqs. (A1) and (A2) results the following relationship used in the text:

$$\begin{aligned}&M_{l\kappa}^{1/2}(l\kappa|L-\omega^2|l'\kappa')M_{l'\kappa'}^{1/2}\\&\quad=M_\kappa^{1/2}(l\kappa|L_0+\Lambda(\omega^2)-\omega^2|l'\kappa')M_{\kappa'}^{1/2}.\end{aligned} \tag{A5}$$

L_0 denotes the unperturbed dynamical matrix and M_κ the mass of the κth ion in the elementary cell of the perfect crystal. (M_0 in matrix notation). $\Lambda(\omega^2)$ is the frequency-dependent perturbation which includes the change of force constants $\delta\Phi\equiv\Phi-\Phi_0$ as well as the mass change δM. $\Lambda(\omega^2)$ reads

$$\begin{aligned}&(\kappa l|\Lambda(\omega^2)|l'\kappa')\\&\quad=M_\kappa^{-1/2}(\kappa l|(\delta\Phi-\omega^2\delta M)|l'\kappa')M_{\kappa'}^{-1/2}.\end{aligned} \tag{A6}$$

Φ_0 is the force-constant matrix of the perfect lattice.

In order to take advantage of defect symmetry properties, we introduced a new basis in the linear vector space. Let α denote the irreducible representation of the point group according to which symmetry coordinates of the imperfect lattice transform. The label I specifies the region of the linear vector space spanned by $\Lambda(\omega^2)$, and II denotes the remaining space. Then, $|\mathrm{I};\alpha j)$ or $|\mathrm{II};\alpha j')$ represent, in region (I) or (II), respectively, the symmetry vectors that transform according to the αth irreducible representation (irr. rep.). j labels the linearly independent vectors of the same irr. rep. $|\mathrm{I};\alpha j)$ and $|\mathrm{II};\alpha j)$ are normalized according to

$$(j\alpha;\mathrm{I}|\mathrm{I};\alpha j')=\delta_{jj'},\quad(j\alpha;\mathrm{II}|\mathrm{II};\alpha j')=\delta_{jj'}. \tag{A7}$$

The perturbed projected density of states is defined by[9]

$$\begin{aligned}\rho_{\alpha jj'}(\omega^2)&=(j\alpha|\,\delta(\omega^2-L_0-\Lambda(\omega^2))|\alpha j')\\&=-(1/\pi)\,\mathrm{Im}(j\alpha|(I-\mathcal{G}^0(\omega^2+i0^+)\Lambda(\omega^2))^{-1}\\&\qquad\times\mathcal{G}^0(\omega^2+i0^+)|\alpha j').\end{aligned} \tag{A8}$$

We understood in Eq. (A8) either label I or II, which can be restored according to which linear vector space region we are considering. Similarly, the unperturbed projected density reads

$$\begin{aligned}\rho_{\alpha jj'}{}^0(\omega^2)&=(j\alpha|\,\delta(\omega^2-L_0)|\alpha j')\\&=-(1/\pi)\,\mathrm{Im}(j\alpha|\,\mathcal{G}^0(\omega^2+i0^+)|\alpha j').\end{aligned} \tag{A9}$$

In the above expression, $\mathcal{G}^0(\omega^2+i0^+)\equiv(\omega^2+i0^+-L_0)^{-1}$ denotes the unperturbed propagator or Green-function matrix, which in the lattice-displacement representation reads

$$\begin{aligned}(\kappa l|\,\mathcal{G}^0(z)\,|l'\kappa')&=(\kappa l|(z-L_0)^{-1}|l'\kappa')\\&=\frac{1}{N}\sum_{s,\mathbf{q}}(z-\omega_{\mathbf{q}s}{}^2)^{-1}\boldsymbol{\varepsilon}_{\mathbf{q}s}(\kappa)\boldsymbol{\varepsilon}_{\mathbf{q}s}{}^*(\kappa')\\&\qquad\times\exp[i\mathbf{q}\cdot(\mathbf{x}_l-\mathbf{x}_{l'})],\end{aligned} \tag{A6}$$

where $z=\omega^2+i\eta$ is the complex squared frequency. $\mathbf{q}$ stands for the wave vector inside the Brillouin zone (B.Z.), s designates the vibrational branch; $\omega_{\mathbf{q}s}{}^2$ and $\boldsymbol{\varepsilon}_{\mathbf{q}s}(\kappa)$ are, respectively, the eigenvalues and eigenvectors of the dynamical matrix $L_0(\mathbf{q})$ in wave vector representation. $\mathbf{x}_l$ is the Bravais lattice vector.

We are particularly interested in the properties of the perturbed projected density of states for region (I). If the irr. rep. α is contained singly in $\Lambda(\omega^2)$, we obtain

$$\rho_\alpha(\omega^2)=\frac{\rho_\alpha{}^0(\omega^2)}{[1-\tilde{\rho}_\alpha{}^0(\omega^2)\Lambda_\alpha(\omega^2)]^2+[\pi\rho_\alpha{}^0(\omega^2)\Lambda_\alpha(\omega^2)]^2}, \tag{A8'}$$

where $\Lambda_\alpha(\omega^2)$ is the αth component of $\Lambda(\omega^2)$, and $\tilde{\rho}_\alpha{}^0(\omega^2)$ the Hilbert transform of $\rho_\alpha{}^0(\omega^2)$, i.e.,

$$\tilde{\rho}_\alpha{}^0(\omega^2)=\int 2\omega' d\omega' \left(\frac{1}{\omega^2-\omega'^2}\right)_P \rho_\alpha{}^0(\omega^2). \quad \text{(A9')}$$

Notice that the contribution to $\rho_\alpha(\omega^2)$, coming from a single defect, is of the same magnitude as that coming from the whole perfect lattice. This is because the symmetry vectors are normalized to unity in subspace (I), [see Eq. (A7)], while the host-lattice normal modes are normalized to unity in the whole crystal space, [see Eq. (A3)]. When the irr. rep. α appears more than one time in $\Lambda(\omega^2)$, the perturbed projected density of states can be written in spectral representation as

$$\rho_\alpha(\omega^2)=-\left(\frac{1}{\pi}\right)\mathrm{Im}\left\{\sum_m |v_{\alpha m}) \times \frac{\mu_{\alpha m}(\omega^2+i0^+)}{\Lambda_{\alpha m}(\omega^2)[1-\mu_{\alpha m}(\omega^2+i0^+)]}(v_{\alpha m}|\right\}, \quad \text{(A10)}$$

where $\mu_{\alpha m}(z)$ and $|v_{\alpha m})$ are, respectively, the eigenvalues and eigenvectors of $\mathcal{G}_\alpha{}^0(z)\Lambda_\alpha(\omega^2)$ (see Refs. 44 and 45) and $\Lambda_{\alpha m}(\omega^2)$ is given by

$$\Lambda_{\alpha m}(\omega^2)=(v_{\alpha m}|\Lambda(\omega^2)|v_{\alpha m}). \quad \text{(A11)}$$

In the above expression, we have omitted the matrix indices j and j' in $\rho_\alpha(\omega^2)$.

Let $\omega_{\alpha R}$ denote the frequency for either a local or pseudolocal mode. $\rho_\alpha(\omega^2)$ splits as

$$\rho_\alpha(\omega^2)=-\left(\frac{1}{\pi}\right)\mathrm{Im}\left\{|v_{\alpha R}) \times \frac{\mu_{\alpha R}(\omega^2+i0^+)}{\Lambda_{\alpha R}(\omega^2)[1-\mu_{\alpha R}(\omega^2+i0^+)]}(v_{\alpha R}|\right\} - (1/\pi)\,\mathrm{Im}\{(\text{n.R.})_\alpha\}, \quad \text{(A12)}$$

where the second term represents the sum of all of the nonresonant (n.R.) modes of α symmetry. At resonance frequency, $|v_{\alpha R})$ turns out to be essentially a real vector (this is exactly true for local and gap modes). As $\mathrm{Im}\mu_{\alpha R}$ can be considered as infinitesimal quantity, Eq. (A12) can be written as

$$\rho_\alpha(\omega^2)=\sum_R \rho_\alpha{}^R(\omega^2)+\rho_\alpha{}^c(\omega^2), \quad \text{(A13)}$$

where

$$\rho_\alpha{}^R(\omega^2)\simeq\frac{1}{|\Lambda_{\alpha R}(\omega_R{}^2)\,\mathrm{Re}\mu_{\alpha R}{}'(\omega_R{}^2)|} \times |v_{\alpha R})\delta(\omega^2-\omega_{\alpha R}{}^2)(v_{\alpha R}|. \quad \text{(A14)}$$

A prime on $\mu_{\alpha R}(\omega^2)$ means first-order derivative with respect to ω^2. In the Eq. (A13) $\sum_R \rho_\alpha{}^R(\omega^2)$ denotes the sum of all the δ-type terms coming from local and pseudolocal modes of α symmetry; $\rho_\alpha{}^c(\omega^2)$ represents the difference

$$\rho_\alpha(\omega^2)-\sum_R \rho_\alpha{}^R(\omega^2). \quad \text{(A15)}$$

$\rho_\alpha{}^c(\omega^2)$ does not have δ-type discontinuities and in fact it represents the remainder of the perturbed projected density of states resulting after both the local and the pseudolocal modes have been separated. We call $\rho_\alpha{}^c(\omega^2)$ the projected density of states of the perturbed vibrational continuum.

It is easy to verify that

$$\int_0^\infty d\omega\; 2\omega\rho_{\alpha jj'}{}^0(\omega^2)=(j\alpha|\alpha j')=\delta_{jj'} \quad \text{(A16)}$$

represents the normalization of $\rho_\alpha{}^0(\omega^2)$. The normalization of $\rho_{\alpha jj'}(\omega^2)$ turns out to be

$$\int_0^\infty d\omega\; 2\omega\rho_{\alpha jj'}(\omega^2)=(j\alpha|M_0M^{-1}|\alpha j'), \quad \text{(A17)}$$

where M_0 and M denote the mass matrices for perfect and imperfect lattices, respectively; Eq. (A17) becomes a Kronecker's δ when either $(\kappa l|\alpha j)$ or $(\kappa' l'|\alpha j')$ does not involve the lattice site in which the change of mass occurred. If a local mode of α symmetry; for instance $|\psi_{\alpha R})$, exists in the imperfect-lattice dynamics, we have

$$\int_0^\infty d\omega\; 2\omega\rho_{\alpha jj'}{}^R(\omega^2)=|(j\alpha|M_0{}^{1/2}M^{-1/2}|\psi_{\alpha R})|^2. \quad \text{(A18)}$$

When the symmetry vector $|\alpha j)$ points in the resonance direction, i.e., $|\alpha j)=|v_{\alpha R})$, it follows that

$$|(v_{\alpha R}|\psi_{\alpha R'})|^2=(1/|\Lambda_{\alpha R}(\omega_R{}^2)\,\mathrm{Re}\mu_{\alpha R}{}'(\omega_R{}^2)|). \quad \text{(A19)}$$

Although with a lesser accuracy, this relation continues to hold also for a sharp pseudolocal mode. It is a valid help in estimating the actual localization of the mode.

[44] M. V. Klein, Phys. Rev. **131**, 1500 (1963); **141**, 716 (1966).
[45] M. Wagner, Phys. Rev. **136**, B562 (1964).